

Cellulose in atmospheric particulate matter at rural and urban sites across France and Switzerland

Adam Brighty^{1,a}, Véronique Jacob¹, Gaëlle Uzu¹, Lucille Borlaza¹, Sébastien Conil²,
Christoph Hueglin³, Stuart K. Grange^{3,4}, Olivier Favez^{5,6}, Cécile Trébuchon⁷, and Jean-Luc
Jaffrezo¹

¹University Grenoble Alpes, CNRS, IRD, INP-G, IGE (UMR 5001), 38000 Grenoble, France

²ANDRA, DRD/GES Observatoire Pérenne de l'Environnement, 55290 Bure, France

³Empa, Swiss Federal Laboratories for Materials Science and Technology, Überlandstrasse 129, 8600 Dübendorf, Switzerland

⁴Wolfson Atmospheric Chemistry Laboratories, University of York, York, YO10 5DD, United Kingdom

⁵Institut national de l'environnement industriel et des risques (INERIS), Parc Technologique Alata BP2, 60550 Verneuil-en-Halatte, France

⁶Laboratoire Central de Surveillance de la Qualité de l'Air (LCSQA), 60550 Verneuil-en-Halatte, France

⁷Atmo AURA, F-38400 Grenoble, France

^a now at: Centre for Environmental Policy, Imperial College London, Weeks Building, SW7 1NE

Correspondance: Adam Brighty (adam.brighty1@gmail.com) and Jean-Luc Jaffrezo (Jean-luc.Jaffrezo@univ-grenoble-alpes.fr)

Abstract

The spatiotemporal variations of free cellulose concentrations in atmospheric particles, as a proxy for plant debris, were investigated using an improved protocol with an HPLC-PAD method. Filter samples were taken from nine sites of varying characteristics across France and Switzerland, with sampling covering all seasons. Concentrations of cellulose, as well as carbonaceous aerosol and other source-specific chemical tracers (e.g. Elemental Carbon (EC), levoglucosan, polyols, trace metals, and glucose) were quantified. Annual mean free cellulose concentrations within PM₁₀ ranged from 29 ± 38 ng m⁻³ at Basel (urban site) to 284 ± 225 ng m⁻³ at Payerne (rural site). Concentrations were considerably higher during episodes, with spikes exceeding 1150 and 2200 ng m⁻³ at Payerne and ANDRA-OPE (rural site), respectively. A clear seasonality, with highest cellulose concentrations during summer and autumn, was

36 observed at all rural and some urban sites. However, some urban locations exhibited a
37 weakened seasonality. Contributions of cellulose-carbon to total organic carbon are moderate
38 on average (0.7 - 5.9 %), but much greater during 'episodes', reaching close to 20% at Payerne.
39 Cellulose concentrations correlated poorly between sites, even a ranges of about 10 km,
40 indicating the localised nature of the sources of atmospheric plant debris. With regards to these
41 sources, correlations between cellulose and typical biogenic chemical tracers (polyols and
42 glucose) were moderate to strong (R_s 0.28 – 0.78, $p < 0.0001$) across the nine sites. Seasonality
43 was strongest at sites with stronger biogenic correlations, suggesting the main source of
44 cellulose arises from biogenic origins. A second input to ambient plant debris concentrations
45 was suggested via resuspension of plant matter at several urban sites, due to moderate cellulose
46 correlations with mineral dust tracers, Ca^{2+} and Ti metal (R_s 0.28 – 0.45, $p < 0.007$). No
47 correlation was obtained with the biomass burning tracer (levoglucosan), an indication that this
48 is not a source of atmospheric cellulose. Finally, an investigation into the interannual variability
49 of atmospheric cellulose across the Grenoble metropole area was completed. It was shown that
50 concentrations and sources of ambient cellulose can vary considerably between years. All
51 together, these results deeply improve our knowledge on the phenomenology of plant debris
52 within ambient air.

53

54 **1. Introduction**

55 Ambient aerosols are a key component of our atmospheric system, with complex compositions
56 arising from multiple sources and formation mechanisms. These airborne particles (or
57 particulate matter, PM) have both climatic and health effects which remain poorly understood
58 (Boucher et al., 2013). Particulate matter is made up of elemental and inorganic material, as
59 well as a significant proportion of material of a carbonaceous nature (organic carbon, OC, and
60 elemental carbon, EC) (Hansen et al., 1984; Birch and Cary, 1996; Putaud et al., 2004a; Yttri
61 et al., 2007a; Franke et al., 2017). PM contains an important portion of organic matter (OM),
62 the chemical composition of which remains largely unidentified (Putaud et al., 2010). In the
63 majority of studies, at most 20% of the OM can be speciated and quantified at the molecular
64 level (Alfarra et al., 2007; Michoud et al., 2021). Understanding the sources and atmospheric
65 mechanisms of this OM fraction remains key to uncovering more knowledge of its climatic
66 and health effects, on both local and larger scales (Nozière et al., 2015). Indeed, it has been
67 hypothesised that our current understanding does not account for a number of hidden sources
68 and processes of PM (Karagulian et al., 2015; Wagenbrenner et al., 2017; Klimont et al., 2017).

69

70 A large proportion of research in the last two decades has been focussed on the production of
71 secondary organic aerosol (SOA) arising from the processing of volatile organic compounds
72 (VOCs), or intermediate/semi-volatile ones (I/SVOCs). So far, a smaller effort has been made
73 to account for the potential additional input from primary biological aerosol particles (PBAP –
74 also known as Primary Biogenic Organic Aerosol, PBOA). However, the limited number of
75 available studies show that a significant portion of OM can be associated with biogenic
76 emissions (Liang et al., 2015; Alves, 2017; Samaké et al., 2019a). PBAP are emitted directly
77 into the atmosphere from the source material, and are described as “solid airborne particles
78 derived from biological organisms, including microorganisms and fragments of biological
79 materials such as plant debris and animal dander” (Després et al., 2012). PBAP aerodynamic
80 diameters can vary greatly based on the source: ranging from a few nanometres (e.g. viruses
81 and cell fragments), to $> 100 \mu\text{m}$ (plant debris, fungal spores, pollen) (Pöschl, 2005). In terms
82 of their atmospheric significance, some forms of PBAP have been shown to be very efficient
83 ice nuclei and giant cloud condensation nuclei, in regions where anthropogenic sources do not
84 dominate emissions (Rosenfeld et al., 2008; Pöschl, 2010). Biological particles have also been
85 linked with acute respiratory effects (e.g. asthma), allergies, and cancer (Peccia et al., 2011).
86 Estimations of global PBAP natural emissions are in the broad range of 50 – 1000 Tg/yr,
87 highlighting the need for further studies to produce more precise estimates (Penner et al., 2001;
88 Jaenicke, 2005). For comparison, global anthropogenic emissions of PM_{10} via road transport,
89 amount to about 3.3 Tg/yr (Klimont et al., 2017),

90

91 Within modern field studies, characterisation of PM is simplified with the use of chemical
92 tracers (also referred to as molecular markers) as proxy species. Such species should be
93 persistently emitted from a given source and sufficiently stable in the atmosphere to be
94 characterised and quantified. The use of these tracers can also lead to more constrained source
95 apportionment calculations, owing to decreased uncertainties and a stronger statistical output,
96 together with a better understanding of the emission processes (Waked et al., 2014; Weber et
97 al., 2019; Borlaza et al., 2021).

98

99 Plant debris (e.g. air-dispersed seeds or plant fragments via abrasion or decomposition
100 mechanisms) is suspected to be a major contributor to PBAP within the atmosphere (Graham
101 et al., 2003; Winiwarter et al., 2009; Martin et al., 2010; Yttri et al., 2011b; Bozzetti et al.,
102 2016;). However, atmospheric plant debris has received much less attention than other sources

103 of PBAP, such as fungal spores, and thus knowledge of plant debris is severely limited. Both
104 cellulose and plant waxes (as n-alkanes) have been used as proxy species for atmospheric plant
105 debris. Early studies of the fraction of plant debris (or vegetative detritus) centred around
106 analysis of plant waxes as the proxy species (Simoneit and Mazurek, 1982; Rogge et al., 1993a;
107 Rogge et al., 1993b). These studies have formed the basis of our work, using identifiable
108 chemical species to supply information on insoluble components. For example, Rogge et al.
109 (1993a) in their experiment found significant amounts of non-extractable, insoluble organic
110 components, yet were able to identify soluble components, such as plant waxes, as chemical
111 tracers for insoluble components, such as plant debris. Rogge et al. (1993a) found local
112 differences in the n-alkanes observed pattern, as a function of the variability in local plant
113 composition, whilst Simoneit and Mazurek (1982) found plant wax to be a major component
114 of rural OC.

115

116 As scientific understanding increased, cellulose was proposed as a new chemical tracer for
117 plant debris by Kunit and Puxbaum (1996) and has been used a tracer in several field and PMF
118 studies since (Tenze-Kunit and Puxbaum, 2003; Sánchez-Ochoa et al., 2007; Caseiro, 2008;
119 Yttri et al., 2011a.; Yttri et al., 2011b; Bozzetti et al., 2016; Borlaza et al., 2021a). Interestingly,
120 Kotianová et al. (2008) evaluated the use of both plant waxes and cellulose as plant debris
121 tracers. They found a much weaker seasonal pattern with respect to cellulose concentrations,
122 but showed plant wax/n-alkane concentrations peaked significantly during the warm summer
123 months. The authors hypothesised that the difference between the two tracers revolved around
124 plant waxes coming from the plant surface, whereas cellulose originating from bulk plant
125 material. As such, atmospheric cellulose is predicted to be derived from machining and
126 decomposition processes, and n-alkanes are emitted as part of surface abrasion mechanisms.
127 Kotianová et al. (2008) found very good agreement in the results between the contributions of
128 both cellulose and plant wax to PM₁₀.

129

130 Studies of other molecular markers are more prominent, both within the primary biogenic
131 fraction and other aerosol classes. The number of campaigns investigating measurements of
132 atmospheric cellulose are scarce in comparison and do not sufficiently cover all ambient
133 environments (Alves, 2017, and references therein). This remains a concern, especially
134 considering that contributions of cellulose-derived carbon (cellulose-C) to overall organic
135 carbon in the atmosphere can be significant during some periods of the year (Sánchez-Ochoa
136 et al., 2007; Caseiro, 2008).

137

138 Cellulose is present as two forms within global flora: firstly as “free cellulose”, and also as
139 cellulose embedded in lignin or hemicellulose. This portion of cellulose bound to lignin
140 requires an additional delignification process before quantification in atmospheric PM, which
141 requires harsh conditions and long reaction times (Gould, 1984; Kunit and Puxbaum, 1996). A
142 conversion from free to total cellulose concentrations was created by Tenze-Kunit and
143 Puxbaum (2003), where free cellulose was shown to contribute 72% of total cellulose
144 abundance. This conversion presents large uncertainties, as it was developed using a very
145 limited sample size ($n < 10$). Thus, free cellulose is commonly used as the proxy species for
146 atmospheric plant debris, over total cellulose.

147

148 Of the few previous characterisation studies to have taken place, only two have had a duration
149 longer than one year. Regardless, some insights into the seasonal variations of cellulose
150 concentrations have been afforded (Sánchez-Ochoa et al., 2007; Caseiro, 2008; Yttri et al.,
151 2011a; Yttri et al., 2011b). For example, Sánchez-Ochoa et al. (2007) highlighted a pattern of
152 cellulose concentration maxima during spring and summer at their rural background sites,
153 excluding their maritime counterparts. This seasonal pattern, however, was found to be much
154 weaker than other aerosol classes and showed higher winter concentrations than anticipated.
155 Further, Caseiro (2008) found winter maxima at close to half their monitoring locations when
156 observing from both urban and background locations. The reasons for the difference in
157 seasonality between these two studies are likely to be owing to the differences in location and
158 the variety of PM sizes used (PM_2 to PM_{10}) by Sánchez-Ochoa et al. (2007) compared to the
159 consistent PM_{10} sampling used by Caseiro (2008). More long-term studies would be beneficial
160 to understanding these geographical discrepancies.

161

162 The lack of sufficient long-term studies and clarity regarding cellulose characterisation of
163 concentrations, seasonal cycles, sources, and emissions processes calls for further
164 measurements. This would enable a better comprehension of the importance of this fraction of
165 PBOA in atmospheric PM. In this study, we present a multi-seasonal investigation of cellulose
166 concentrations alongside other chemical tracers in ambient aerosol, collected at nine sites
167 across both France and Switzerland. The objective of the study was to investigate the seasonal
168 and geographical variability of atmospheric cellulose across sites of varying characteristics.
169 Contributions of cellulose to the OM fraction of PM, and correlations of cellulose with tracers
170 of characteristic sources were also completed, alongside the creation of a biannual and triannual

171 dataset of cellulose concentrations at three sites within the Grenoble metropole and at ANDRA-
172 OPE (both France), respectively. Further, a $PM_{2.5}/PM_{10}$ intercomparison was also established.
173 This study, with the gathering of one of the largest data bases on atmospheric cellulose with
174 more than 1500 samples, aims to provide a better understanding of this understudied
175 component of atmospheric PM.

176

177 **2. Experimental**

178 **2.1 Sampling Sites**

179

180 PM samples used for the present study have been collected during three distinct projects, which
181 are described in the following. The locations of the corresponding measurement sites are
182 presented on Fig. 1a and b, while site classifications, sampling periods, and numbers of
183 available samples are summarised in Table 1 and Table 2.

184

185 The first measurement campaign (QAMECS) focused on the PM_{10} loading and composition
186 at various sites within the Grenoble metropole (France), as part of the Mobil’Air air quality
187 programme (Borlaza et al., 2021a,b). In these campaigns, three sites were monitored over two
188 one-year periods (2017 – 2018, 2020 – 2021). As the largest metropolis in the Alps, Grenoble
189 is home to around 450,000 inhabitants. The city itself is situated within an alpine valley: the
190 centre is at relatively low altitude (between 200 and 600 metres above sea level) and is
191 surrounded by multiple separate mountain ranges, namely Chartreuse (to the north),
192 Belledonne (east) and Vercors (south and west). These ranges heavily inhibit horizontal air
193 movement, leading to unique meteorological conditions and favouring the formation of
194 temperature inversions, trapping pollutants within the valley, especially during winter. During
195 this study, a PM_{10} sampling campaign was undertaken in the Grenoble metropole at three sites,
196 each representing a different urban site typology: Les Frênes (LF, urban background), Vif
197 (peri-urban) and Caserne de Bonne (CB, urban centre). All three sites are within 15 km of one
198 another (Fig. 1b).

199 Secondly, PM_{10} and $PM_{2.5}$ samples could be obtained from a monitoring campaign at the
200 Observatoire Pérenne de l’Environnement (ANDRA-OPE), in northern France
201 (<http://ope.andra.fr/index.php?>). Samples have been collected continuously for about a decade
202 at this site (Golly et al., 2019; Borlaza et al., 2021c) but cellulose measurements were
203 conducted and presented in this work for the years 2016, 2017 and 2020, only. PM_{10} and $PM_{2.5}$

204 samples were taken on alternate days. The ANDRA-OPE site is situated 230 km east of Paris,
 205 on a rise in between lows of the Paris Basin and the mountains in the department of Les Vosges
 206 (OPE-ANDRA Atmospheric Station). It is subject to persistent westerly prevailing winds and
 207 is surrounded by significant agricultural activities but is notably distant from towns (> 25 km)
 208 and small villages (> 4 km).

209 Last but not least, simultaneous PM₁₀ and PM_{2.5} filter samples were taken across five sites in
 210 Switzerland, as part of an EMPA monitoring campaign (Grange et al., 2021). These sites varied
 211 in characteristics and were sampled for one year (from June 2018 to May 2019). Two rural
 212 sites, Magadino and Payerne, are included within the study. The former is located south of the
 213 Alps, whilst the latter is found on the Northern plateau roughly 50 km from the nearest city of
 214 Bern. Filter samples were also taken from urban sites within three of the most populous cities
 215 in Switzerland: Basel, Bern and Zurich. Zurich has a similar topography to the Grenoble
 216 metropole, whilst the traffic-impacted site in Bern resides within a ‘street canyon’, thus both
 217 sites may also experience inhibited air movement. The monitoring site in Basel is within a
 218 suburban area, located in an open and park-like environment. It is not expected to be impacted
 219 by accumulation effects.

Table 1: Sampling period and site characteristics for the PM₁₀ sampling campaign. LF = Les Frênes, CB = Caserne de Bonne. LF, CB and VIF represent sites from the Grenoble metropole.

Site	PM Size, μm	Site Type	Sampling Start	Sampling Finish	# Samples
LF	10	Urban	28/02/2017	31/03/2018	286
		Background	02/01/2020	12/03/2021	
Vif	10	Peri-urban	28/02/2017	31/03/2018	218
			30/06/2020	12/03/2021	
CB	10	Urban	28/02/2017	10/03/2018	209
			30/06/2020	12/03/2021	
ANDRA-OPE	10	Rural background	04/01/2016	27/12/2017	174
			04/01/2020	29/12/2020	
Zurich	10	Urban	03/06/2018	29/05/2019	88
Payerne	10	Rural	03/06/2018	29/05/2019	90
Basel	10	Suburban	03/06/2018	29/05/2019	90
Magadino	10	Rural	03/06/2018	29/05/2019	90
Bern	10	Urban-traffic	03/06/2018	29/05/2019	89

Table 2: Sampling period and site characteristics for the PM_{2.5} sampling campaign

Site	PM Size / μm	Site Type	Sampling Start	Sampling Finish	# Samples
ANDRA-OPE	2.5	Rural Background	01/01/2020	26/12/2020	51
Zurich	2.5	Urban	03/06/2018	29/05/2019	89
Payerne	2.5	Rural	03/06/2018	29/05/2019	90

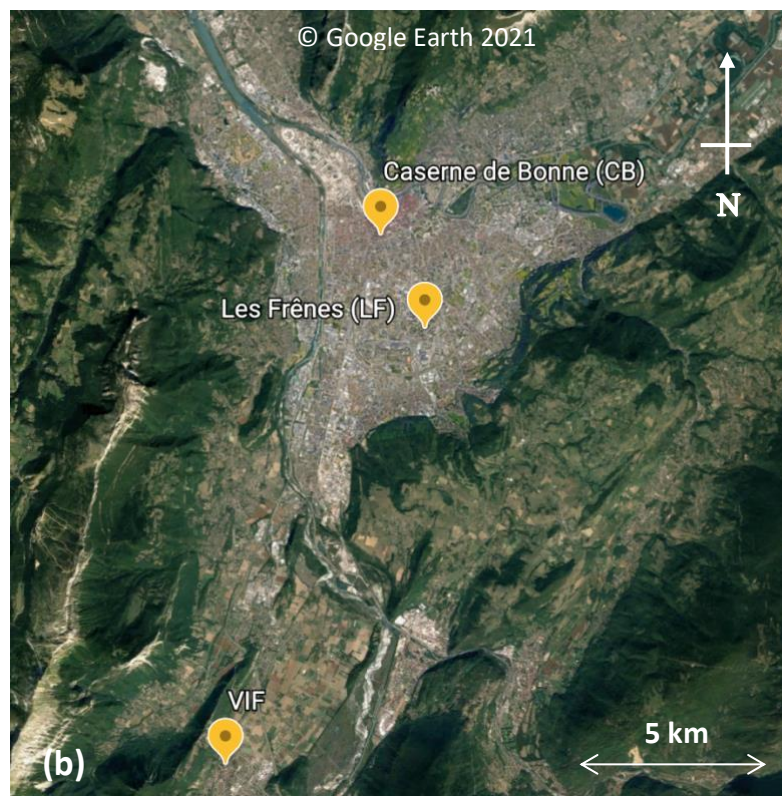
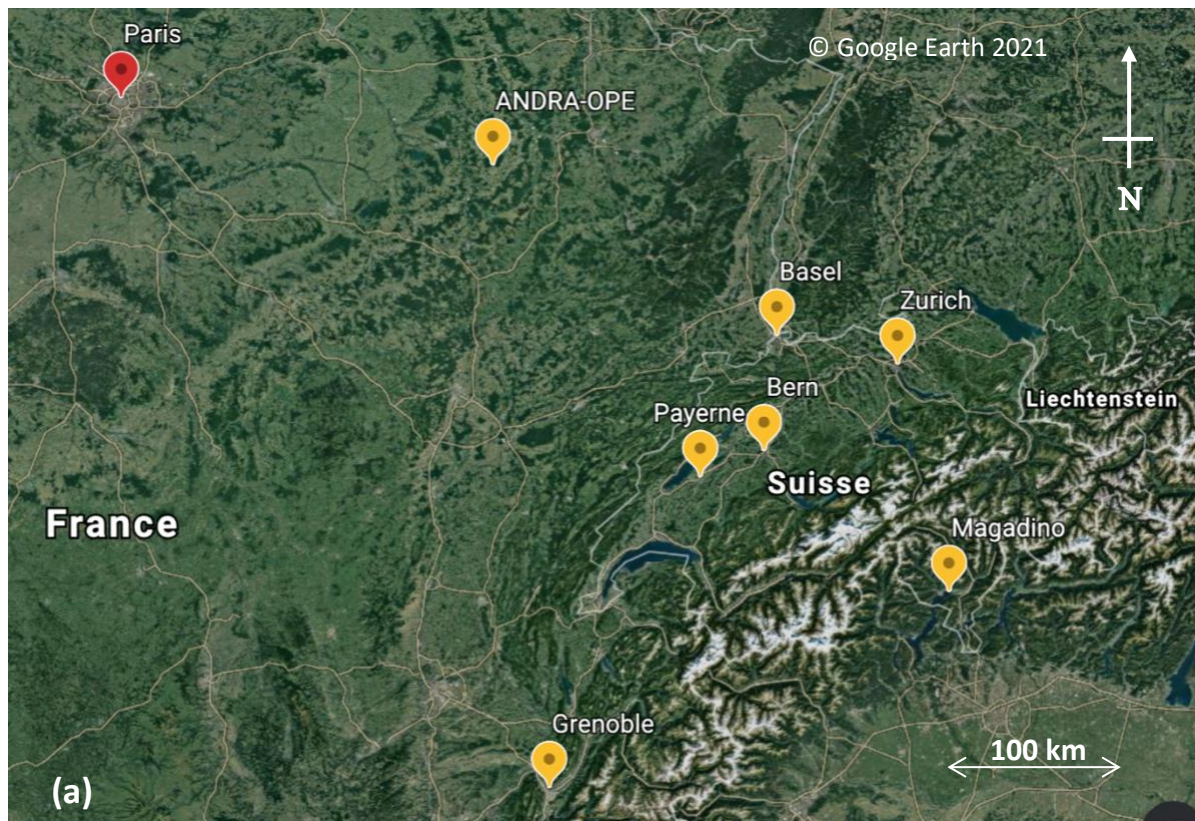


Figure 1. a) A map of all sampling sites from within the study (highlighted with yellow pin drops). Five sites are sampled within Switzerland, three sites within the Grenoble metropole, and one in Northern France – ANDRA-OPE. b) Situation of the three sampling sites within Grenoble.

221 2.2 Sampling Procedure

222

223 At each of the nine sites used for the present study, daily (24-h) PM sample collection periods
224 were conducted according to Table 1 and Table 2 (starting at 00:00 or 09:00 local time) with
225 an average 3-day sampling interval within the Grenoble metropole, 4-day interval for the Swiss
226 sites, and 6-day for the ANDRA-OPE monitoring site. Additional samples for PM₁₀ were
227 collected daily during 9 weeks in summer 2017 in OPE and Grenoble and measured for
228 cellulose, but are not considered in this study (Samaké et al., 2020). The PM collection was
229 performed using high volume samplers (Digitel DA80, 30 m³ h⁻¹) onto 150 mm-diameter pure
230 quartz fibre filters (Tissu-quartz PALL QAT-UP 2500 diameter 150 mm). Excluding the Swiss
231 sites, filters were pre-fired at 500 °C for 12 hours before use to avoid organic contamination,
232 and all were handled under strict quality control procedures. After collection, samples were
233 wrapped in aluminium foil or sterile parchment, sealed in Ziploc plastic bags, and stored at <
234 4 °C until use for chemical analyses. Blank filters were collected to determine detection limits
235 (DL) and to check for the absence of contamination during sample transport, setup, and
236 recovery.

237

238 2.3 Set of Analyses

239

240 All PM₁₀ filters from the nine monitoring locations were analysed for cellulose, while PM_{2.5}
241 filter samples have been analysed at three of the monitoring locations available. The PM₁₀ and
242 PM_{2.5} filter samples were subjected to several other chemical analyses in order to quantify their
243 major chemical components and tracers used in this study.

244

245 Carbonaceous Aerosol

246 Organic carbon (OC) and elemental carbon (EC) were analysed with a Sunset Lab analyser
247 following the EUSAAR2 thermo-optical protocol (Hansen et al., 1984; Birch and Cary, 1996;
248 Aymoz et al., 2007; Cavalli et al., 2010) and according to the recommendations of EN 16909
249 European standard. A punch of 1.5 cm² was used and automatic split time was always selected
250 in order to differentiate between EC and OC.

251

252 Sugar alcohols, anhydrides and glucose

253 Sugar anhydrides (levoglucosan, mannosan and galactosan), sugar alcohols (mannitol, arabitol
254 and sorbitol) and glucose were analysed by High Performance Liquid Chromatography with

255 Pulsed Amperometric Detection (HPLC-PAD) (Waked et al., 2014; Samaké et al., 2019a). A
256 Thermo-Fisher ICS 5000+ HPLC was used with a 4 mm diameter Metrosep Carb 2×150 mm
257 column and 50 mm pre-column in isocratic mode with an eluent of 15% of sodium hydroxide
258 (200 mM), sodium acetate (4 mM) and 85% water, at 1 mL min⁻¹. For this analysis, an
259 extraction was performed upon 5.09 cm² punches soaked in 7 mL of ultra-pure water under
260 vortex agitation for 20 minutes. The extract was then filtered with a 0.25 µm porosity Acrodisc
261 (Milipore Millex-EIMF) filter before analysis.

262

263 Ionic components

264 Quantification of sodium (Na⁺), ammonium (NH₄⁺), potassium (K⁺), magnesium (Mg²⁺),
265 calcium (Ca²⁺), chloride (Cl⁻), nitrate (NO₃⁻), sulfate (SO₄²⁻), and methane sulfonic acid (MSA)
266 was completed using ion chromatography (IC), in agreement with EN 16913. An extraction
267 was performed on 11.34 cm² filter punches in 10 mL of ultra-pure water under vortex agitation
268 for 20 minutes. The extract was then filtered with a 0.25 µm porosity Acrodisc (Milipore
269 Millex-EIMF) filter. The major ionic components were measured by ion chromatography (IC)
270 following a standard protocol described in Jaffrezo et al. (1998) and Waked et al. (2014) using
271 an ICS3000 dual channel chromatograph (Thermo-Fisher) with AS1 IHC column for the anions
272 and CS12 for the cations.

273

274 Major and trace elements

275 Preparation of an extract was completed via mineralisation of a 38 mm diameter filter punch
276 in 5 mL of HNO₃ (70%) and 1.25 mL of H₂O₂ at 180 °C for 30 minutes in a microwave oven
277 (microwave MARS 6, CEM). The analysis of 18 elements (Al, As, Ba, Cd, Cr, Cu, Fe, Mn,
278 Mo, Ni, Pb, Rb, Sb, Se, Sn, Ti, V, and Zn) was performed on each filter extract using
279 inductively coupled plasma mass spectroscopy (ICP-MS) (ELAN 6100 DRC II PerkinElmer
280 or NEXION PerkinElmer) akin to the method described by Alleman et al. (2010).

281

282 Cellulose

283 The concentration of “free” cellulose within the filter samples was determined following an
284 improved protocol based on the enzymatic procedure proposed by Kunit and Puxbaum (1996).
285 Free cellulose was extracted in an aqueous solution, which was then enzymatically hydrolysed
286 to glucose units using two cellulolytic enzymes. The glucose concentration was then quantified
287 by using an HPLC-PAD method. The hydrolysis step was the same as originally proposed,
288 however the enzyme quantities and analytical step have been modified in our protocol.

289 First, a 21 mm diameter punch was soaked in 3 mL of aqueous solution with a thymol buffer
290 (pH 4.8, see supplementary information) and was extracted for 40 minutes in an ultrasound
291 bath. The two enzymes are added into the solution containing the filter: cellulase (from
292 *Trichoderma reesei*, Sigma Aldrich, C2730) with 20 μL of an aqueous solution at 70 units g^{-1}
293 and glucosidase (from *Aspergillus niger*, Sigma Aldrich, 49291), with 60 μL of an aqueous
294 solution at 5 units g^{-1} . The filter-containing solution was then incubated at 50 °C for 24 hours
295 for hydrolysis to occur. Hydrolysis was then terminated by denaturing the enzymes, by placing
296 the solution in an oven at 100 °C for 45 minutes. Finally, the solution was centrifuged (9000
297 rpm) for 15 minutes at 15 °C and carefully separated and extracted from the filter and enzymes,
298 before being analysed with an HPLC-PAD instrument.

299
300 The HPLC-PAD (Dionex DX500) was equipped with a Metrohm column (250 mm long, 4 mm
301 diameter), with an isocratic run of 40 minutes with the eluents A (84%, H_2O), B (14%, 100
302 mM NaOH), and C (2%, 100 mM NaOH + 150mM NaOAc). Column temperature was
303 maintained at 30 °C. Eluent flow rate was 1.10 mL min^{-1} , and injection volume was 250 μL .

304 Each analytical batch contained six glucose and six cellulose hydrolysis standard solutions,
305 alongside unknown samples. Cellulose standards are used to calculate the cellulose-to-glucose
306 hydrolysis efficiency for each batch and are made from cellulose beads of 20 μm (Sigma
307 Aldrich, S3504). The final calculation of the atmospheric concentration of the free cellulose
308 takes this efficiency of conversion into account. The efficiency was variable between batches,
309 but was typically between 75 – 94%, resulting in an average of $85 \pm 8 \%$. The calculation also
310 subtracts the initial concentrations of atmospheric glucose of each sample, determined in
311 parallel with the aforementioned analysis of sugars and polyols. Finally, field and procedural
312 blanks are taken into account. The procedural blank results are greatly improved when the stock
313 cellulase enzyme solution is filtered to lower their glucose content. This is performed through
314 a series of centrifugal cleaning steps ($n=10$) by tangential ultrafiltration in a Vivaspin 15R tube
315 at 9000 rpm in Milli-Q water. Additional procedural information can be found in the
316 supplementary information (SI).

317 **2.4 Cellulose Method Validation**

318 This cellulose quantification method was subjected to a repeatability test, in order to quantify
319 the uncertainties with respect to glucose content within the filter punches. Briefly, a high-
320 volume sampler (Digitel DA80, 30 $\text{m}^3 \text{h}^{-1}$) was used to collect PM_{10} onto a pre-fired quartz

321 fibre filter (Tissu-quartz PALL QAT-UP 2500 diameter 150 mm) on the roof of the laboratory,
322 and sampled a total of 615.1 m³ of air on 15/03/2021. Ten filter punches of 21 mm were then
323 taken and subjected to the same cellulose-to-glucose enzymatic procedure as for normal
324 samples. It is important to state that we assume constant concentrations of both native glucose
325 and cellulose within the filter, as well as the same enzymatic cellulose-to-glucose conversion
326 efficiency for all ten filter punches. Each filter punch was then analysed three times using the
327 same HPLC-PAD method, to monitor repeatability in terms of both cellulose hydrolysis and
328 PAD glucose concentration measurements. Post hydrolysis, the total glucose content of the ten
329 filters was found. The variability (Relative Standard Deviation – RSD) was small, ranging from
330 0.7 – 5.7 % for the three repeats of the same filter sample. The RSD of the glucose content
331 within the ten filter punches was calculated to be 9.9 %. For a 95% confidence in the
332 uncertainty estimate, the uncertainty in the measurement was therefore found to be 20% at a
333 maximum.

334

335 **2.5 Limit of Quantification**

336

337 In order to check for potential contamination of filters during transport, sampling and storage,
338 blank filters were taken across the nine sites. Within the Grenoble metropole, blank filters were
339 taken at Les Frênes and then applied to Caserne de Bonne and Vif (labelled QAMECS in Table
340 3). Further, blank filters were taken at ANDRA-OPE on both PM₁₀ and PM_{2.5} sampling days.
341 With regards to the Swiss sites (EMPA), blanks were taken from each sampling site and an
342 average glucose concentration taken from across the five locations.

343

344 Glucose concentrations calculated in the blanks were then subtracted from measured glucose
345 concentrations within each sample. After, any sample that then yielded a negative
346 concentration of glucose was deemed to be lower than the quantification limit (< QL),
347 representing 5.2 % of all samples. Table 3 summarises the concentrations of cellulose on the
348 blank filters, which has been converted from the blank glucose concentration and the average
349 sampling volume taken across the series. QL varied according to the site, from 0.53 to 13.4 ng
350 m⁻³. In subsequent analyses of monthly, seasonal or annual concentrations (sections 3.1 - 3.3
351 and 3.6), any sample that was deemed < QL was assigned a cellulose concentration of
352 [Blank]/2. This prevents an artificial increase in average cellulose concentrations.

Table 3: Cellulose concentrations derived from blank filters to derive the quantification limit (QL) for each site.

Campaign	QAMECS			EMPA				ANDRA- OPE	
Site	LF	CB	VIF	Basel	Bern	Magadino	Payerne	Zurich	ANDRA
Blank conc ⁿ , ng m ⁻³	7.1	7.1	7.1	0.53	0.53	0.53	0.53	0.53	13.4
No. Field Blanks	3	3	3	5	5	5	5	5	2
No. Samples < QL	14	16	32	14	3	0	0	0	3
% Samples < QL	4.9	7.7	14.7	15.6	3.4	0	0	0	1.7

353 3. Results and Discussion

354

355 In the following, cellulose concentrations are reported as “free” cellulose. The multiplication
 356 factor of 1.39 derived by Tenze-Kunit and Puxbaum (2003) could have been used to derive
 357 “total” cellulose. We chose not to do this, due to the large uncertainty in this ratio. From this
 358 point onwards, “free” cellulose will be regarded as cellulose.

359

360 3.1 Comparison with previous data from the literature

361

362 Figure 2 illustrates the annual averages of cellulose concentrations across our nine sites (in
 363 orange), as well as previous data from the literature (in blue), sorted by site typology and
 364 sampled particle size. The bars represent either annual cellulose averages (if sampling lasted
 365 greater than one year) or cellulose averages for the designated sampling period. We believe
 366 that the roughly 4440 samples (excluding the ones produced within our study) considered in
 367 this literature survey represent the near complete data base of cellulose concentrations in PM
 368 available in the literature. A tabulated version of the results from within the study can be found
 369 in Table 4. An expanded version of Table 4, also including previous literature results, can be
 370 found in Table S1 (SI). The evolution of cellulose concentrations across the respective
 371 sampling periods for our study have further been included in the SI (Fig. S1).

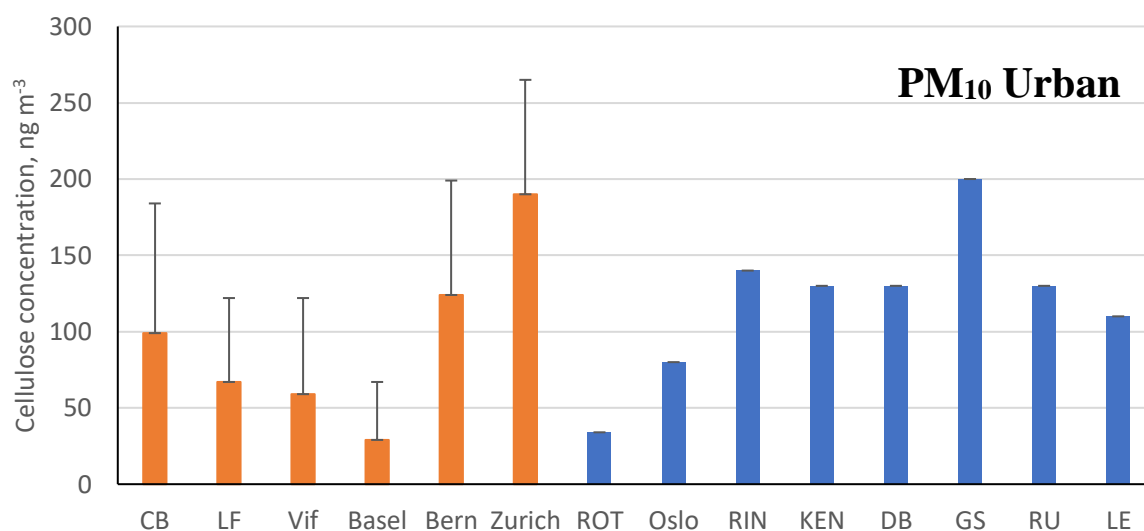
372

373 The concentrations measured in this study are in the same order of magnitude as those reported
 374 in the literature for previous measurement campaigns. This is generally the case for both
 375 seasonal averages and overall maximum concentrations, in both coarse and fine mode aerosol
 376 (Sánchez-Ochoa et al., 2007; Caseiro, 2008; Yttri et al., 2011a; Yttri et al., 2011b). As shown
 377 in Fig. 4, annual cellulose concentrations in PM₁₀ in our study ranged from 29.3 ± 38.4 ng m⁻³
 378 (Bern) to 284.3 ± 224.8 ng m⁻³ (Payerne), and in PM_{2.5} ranged from 15.9 ± 15.0 ng m⁻³

379 (ANDRA-OPE) to $118.1 \pm 76.5 \text{ ng m}^{-3}$ (Payerne). This annual average PM₁₀ cellulose
380 concentration taken at Payerne is higher than any previously recorded in literature by roughly
381 50 ng m^{-3} .

382

383 Moreover, results obtained at Payerne evidenced three episodic (high cellulose concentration)
384 spikes (03/06, 13/07, and 29/07 – highlighted in red, Fig. S1) which exceeded any maximum
385 episode found in literature, by at least 160 ng m^{-3} (Sánchez-Ochoa et al., 2007; Caseiro, 2008;
386 Winiwarter et al., 2009). One striking feature of the overall concentration evolution at Payerne
387 is the high cellulose concentrations at the beginning in June 2018, and the surprisingly low
388 concentrations in April and May 2019 (Fig. S2). Another high concentration episode exceeding
389 those found in literature was documented at the rural site of ANDRA-OPE. The episodic
390 concentration of 2027 ng m^{-3} (07/07/2018 – highlighted in red, Fig. S1) is almost double that
391 of any other measurement, including those generally obtained in the present study. Samaké et
392 al., (2020) recently reported at the same site a noticeable increase in concentrations of PBAP
393 tracers, cellulose included, during harvest in the late summer 2017. However, given the
394 concentration spike in 2018 originated during early July, the middle of the European summer,
395 it is not sure that this new episode can be correlated with agricultural activity.



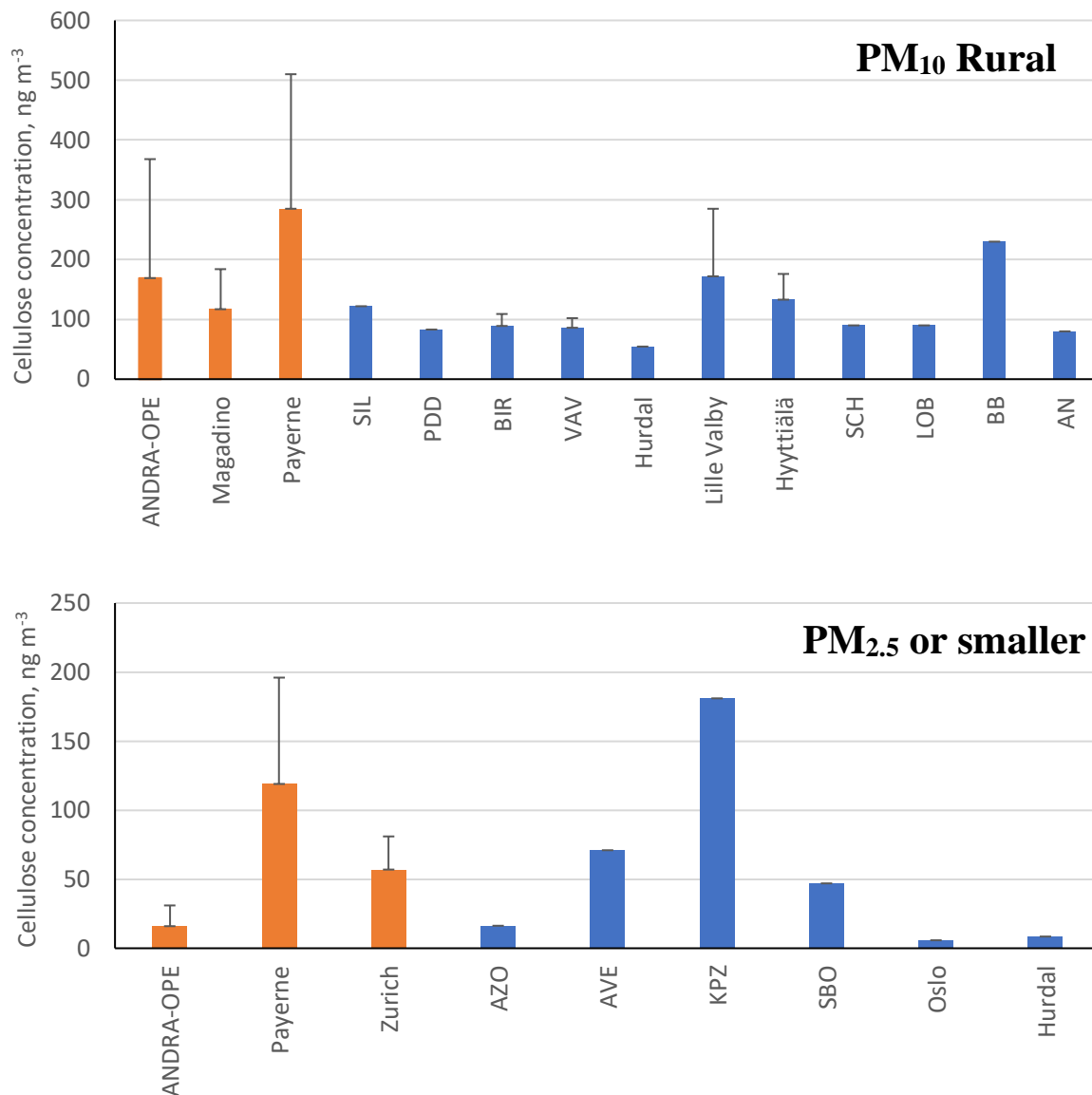


Figure 2: Annual cellulose concentrations (ng m^{-3}) reported within this study (orange bars) alongside previous literature measurements (blue bars). Black bars represent the standard deviation of the results. Bar charts are assigned as follows: Top – urban-based sites; Middle – rural-based sites; Bottom – $\text{PM}_{2.5}$ cellulose measurements (fine mode) or smaller. **Note: Only positive error bars are used for clarity.**

Countries for literature sampling sites:

PM₁₀ Urban: ROT – Netherlands; Oslo – Norway; RIN, KEN, DB, GS, RU and LE – Austria.

PM₁₀ Rural: SIL – Germany; PDD – France; BIR, Hurdal and Hyytiälä – Norway; Lille Valby, VAV – Denmark; SCH, LOB, BB and AN – Austria.

PM_{2.5} or smaller: AZO, AVE – Portugal; KPZ – Hungary; SBO – Austria; Oslo, Hurdal – Norway.

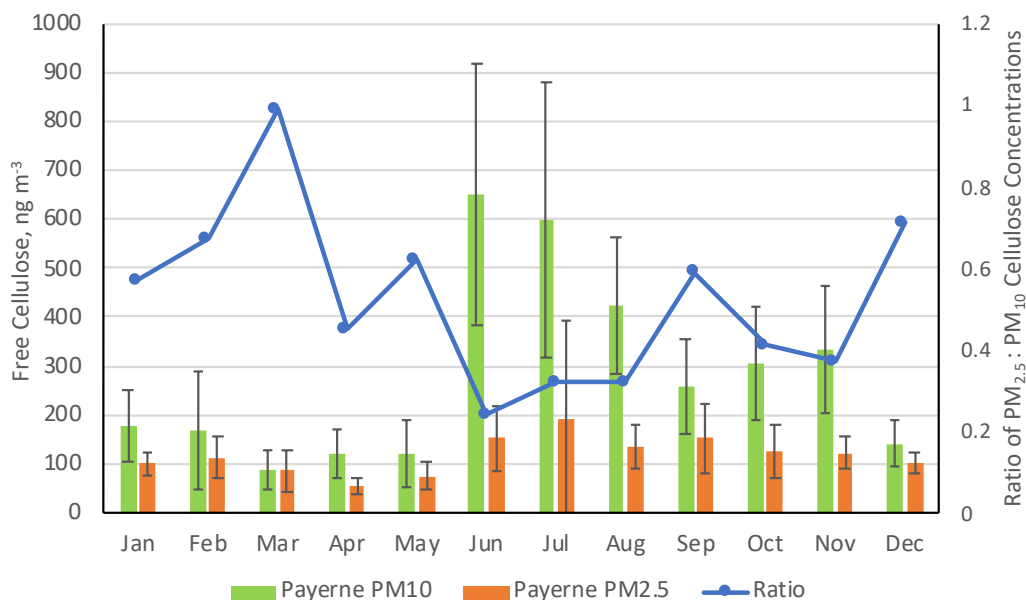
Table 4: Cellulose concentrations (ng m^{-3}) within PM_{10} and $\text{PM}_{2.5}$ across the nine locations studied. Concentrations are shown as annual and seasonal averages (plus 1 σ), as well as the total range of cellulose concentrations seen across the respective period.

Cellulose (ng m^{-3})	Site	Particle Size (μm)	# Samples	Annual		Winter		Spring		Summer		Autumn	
				Mean \pm SD	Range	Mean \pm SD	Range	Mean \pm SD	Range	Mean \pm SD	Range	Mean \pm SD	Range
LF		10	286	67 \pm 55	(1 – 379)	34 \pm 29	(1 – 146)	57 \pm 44	(1 – 214)	98 \pm 58	(29 – 379)	93 \pm 60	(1 – 333)
VIF		10	218	59 \pm 63	(0.0 – 344)	43 \pm 47	(0.0 – 222)	44 \pm 38	(3 – 186)	68 \pm 87	(1 – 344)	77 \pm 65	(1 – 286)
CB		10	206	99 \pm 85	(1 – 701)	85 \pm 111	(1 – 701)	131 \pm 56	(46 – 288)	94 \pm 59	(3 – 238)	95 \pm 85	(3 – 357)
ANDRA-OPE		10	174	169 \pm 199	(3 – 2027)	90 \pm 115	(3 – 518)	102 \pm 116	(12 – 560)	247 \pm 260	(7 – 2027)	90 \pm 67	(13 – 290)
ANDRA-OPE		2.5	51	16 \pm 15	(0.3 – 41)	17 \pm 21	(0.3 – 41)	< LD	< LD	15 \pm 12	(6 – 32)	16 \pm 18	(2 – 40)
Basel		10	90	29 \pm 38	(2 – 266)	27 \pm 57	(2 – 266)	35 \pm 37	(10 – 154)	32 \pm 35	(11 – 179)	23 \pm 16	(3 – 83)
Bern		10	89	124 \pm 75	(25 – 318)	66 \pm 45	(30 – 159)	76 \pm 52	(25 – 241)	143 \pm 45	(99 – 306)	138 \pm 72	(78 – 318)
Magadino		10	90	117 \pm 67	(16 – 348)	53 \pm 23	(17 – 103)	84 \pm 48	(43 – 282)	135 \pm 65	(60 – 348)	131 \pm 54	(48 – 279)
Payerne		10	90	284 \pm 225	(53 – 1194)	163 \pm 84	(90 – 437)	108 \pm 54	(53 – 284)	553 \pm 246	(235 – 1194)	300 \pm 114	(96 – 538)
Payerne		2.5	90	118 \pm 77	(29 – 678)	105 \pm 29	(71 – 201)	74 \pm 33	(29 – 163)	161 \pm 122	(75 – 678)	132 \pm 52	(74 – 275)
Zurich		10	88	190 \pm 75	(7 – 521)	189 \pm 48	(116 – 342)	177 \pm 51	(81 – 260)	197 \pm 71	(7 – 330)	198 \pm 112	(48 – 521)
Zurich		2.5	89	57 \pm 24	(11 – 163)	52 \pm 16	(31 – 89)	52 \pm 26	(13 – 199)	58 \pm 20	(33 – 109)	64 \pm 31	(11 – 163)

396 3.2 Size distribution (PM₁₀ vs PM_{2.5})

397

398 Figure 3 presents the comparative monthly average concentrations of cellulose in PM₁₀ and
399 PM_{2.5} taken at the three sites of Payerne, Zurich, and ANDRA-OPE, respectively (overall
400 concentration evolutions presented in Fig. S2, SI). Cellulose concentrations in PM₁₀ are
401 consistently much higher than those in PM_{2.5}, with annual average in PM_{2.5} representing
402 between 18 and 42 % of that in PM₁₀ for the 3 sites. However, very large fluctuations in this
403 monthly ratio can be observed, particularly for the two rural sites (Payerne and ANDRA-OPE).
404 This is primarily due to changes in PM₁₀ cellulose concentrations, as those within PM_{2.5}
405 remained largely consistent. Further, considering the overall evolution in Fig. S2, episodic
406 PM_{2.5} concentrations still generally remain well below the PM₁₀ cellulose concentrations
407 around the same period. It seems that some process is largely impacting the source strength of
408 atmospheric plant debris within PM₁₀, particularly in the rural sites. In the city of Zurich, the
409 cellulose PM_{2.5}/PM₁₀ ratio remained relatively constant, just like the concentrations
410 themselves. The comparatively low cellulose concentrations at ANDRA-OPE for 2020 (both
411 PM₁₀ and PM_{2.5}) are discussed as part of section 3.7, in the interannual comparison. No ratio is
412 provided at ANDRA-OPE as PM_{2.5} and PM₁₀ measurements were completed on different days,
413 as opposed to simultaneous PM₁₀ and PM_{2.5} sampling at Payerne and Zurich.



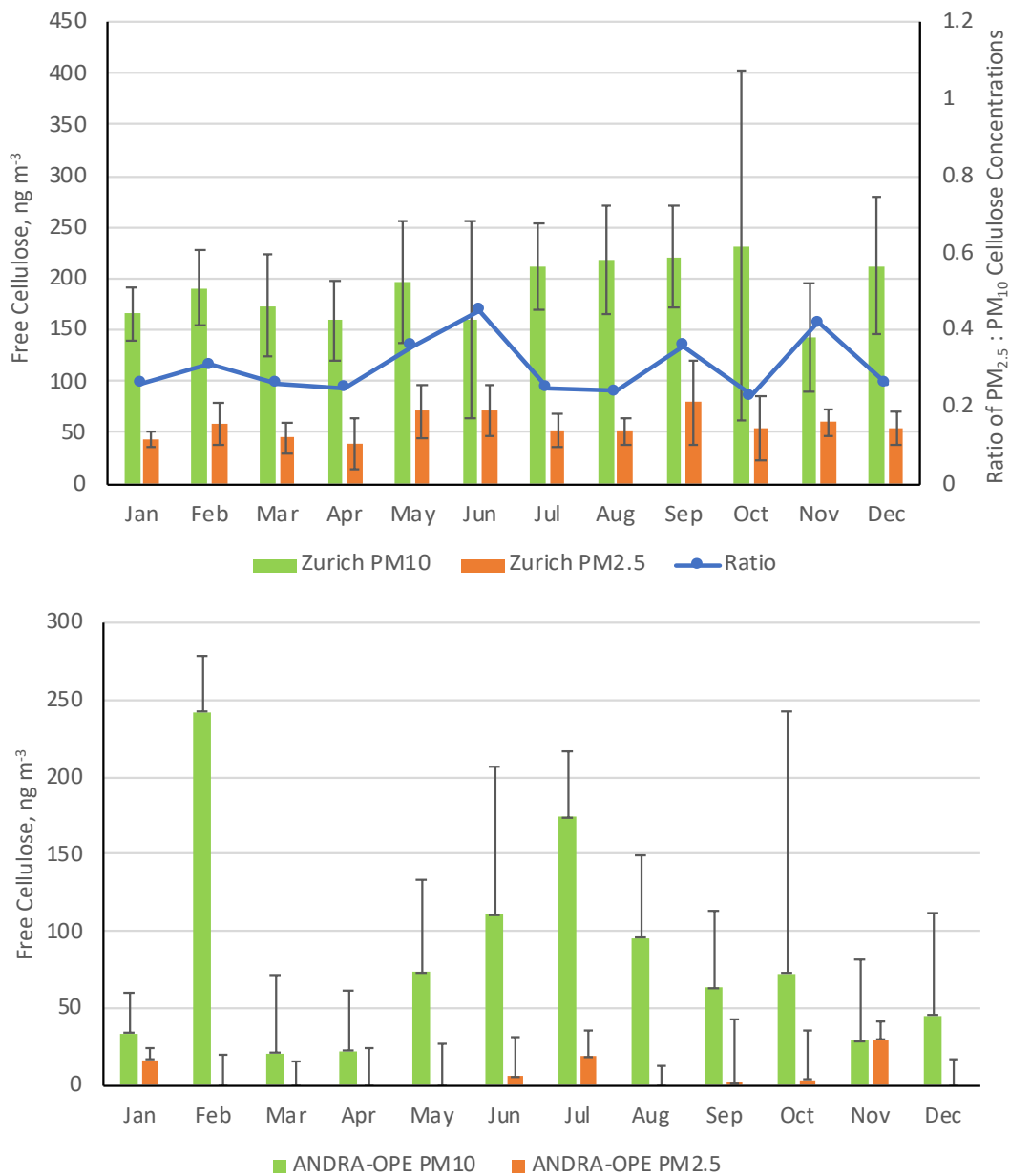


Figure 3: Monthly averages of cellulose concentrations within PM_{10} (green bars) and $PM_{2.5}$ (orange bars) at the three sampling sites of Payerne (rural, top), Zurich (urban, middle) and ANDRA-OPE (rural, bottom). Black error bars represent one standard deviation of the results. The corresponding blue lines represent the ratio of the monthly mean cellulose concentrations in $PM_{2.5}$: PM_{10} . **Note: ANDRA-OPE data is only for the year of 2020, and only positive error bars are used for clarity (StDev larger than mean).**

414 Importantly, across the three sites, less than 30% of atmospheric cellulose was found within
 415 $PM_{2.5}$, on average. This large data set of size resolved cellulose concentrations confirms that
 416 plant debris predominantly resides within the coarse aerosol mode (Sánchez-Ochoa et al., 2007;
 417 Yttri et al., 2011a). Thus, the remainder of this work will solely discuss PM_{10} data to understand
 418 atmospheric cellulose and its behaviour.

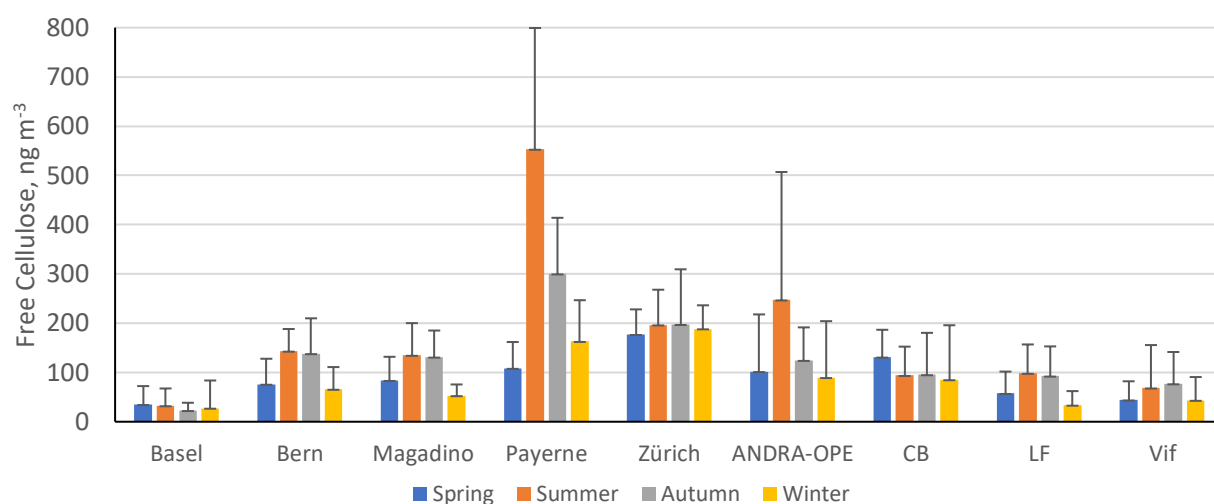
419 3.3 Variations of cellulose concentrations in time and space

420

421 Previous studies indicate either a temporal variation with cellulose concentration maxima
422 during the spring and summer seasons (Sánchez-Ochoa et al., 2007), or show very minimal
423 seasonality (Caseiro, 2008). The following discussion will take these observations into account
424 by presenting the results in terms of seasonal averages. Seasons were defined in three-month
425 periods: Dec – Feb (Winter), Mar – May (Spring), Jun – Aug (Summer), Sep – Nov (Autumn).
426 At the nine sites investigated, our PM₁₀ cellulose measurements were above the limit of
427 detection across all seasons. Figure 4 illustrates these seasonal cellulose concentrations (ng m⁻³)
428 for the nine locations. Numerical values of seasonal means and ranges are tabulated as part
429 of Table S1 (SI).

430

431 In general, the seasonal pattern exhibited here shows higher cellulose concentrations during
432 summer and autumn, likely due to increased temperature and humidity increasing the activity
433 of soil and litter decomposers as well as improving the quality of the litter composition. For
434 example, nitrogen content of leaves is shown to be greater in warmer temperatures, which leads
435 to better conditions for leaf degradation by microbial action (Liu et al., 2006; Verma et al.,
436 2018). It should be stated that this hypothesis would require further experiments, including
437 specific field measurements linking soil and litter state and plant debris emission. The general
438 trend above is exhibited at all rural sites, and some urban locations (Bern, LF, Vif). However,
439 the extent to which these concentrations exceed the other seasons varied greatly. Normalised
440 seasonal concentrations for each site can be found in Fig. S3, to show this variability.
441 Considering this general seasonality, a summer-autumn maximum in cellulose concentrations
442 deviates from the spring-summer maximum suggested by Sánchez-Ochoa et al. (2007). This
443 may be a result of the different particle size fractions measured as part of their sampling
444 campaign (i.e., PM₂, PM_{2.5} or PM₁₀), compared to the consistent PM₁₀ measurements used in
445 this study. This might also be due to the presence of three high altitude, mountainous sites
446 comprised within the six sites investigated by Sánchez-Ochoa et al. (2007). Large standard
447 deviations are also noticed at the two rural sites of ANDRA-OPE and Payerne, especially
448 during the summer months. This implies a significant variability in the source of atmospheric
449 cellulose at these sites, especially when compared to the more urban locations showing smaller
450 standard deviations and therefore a smaller flux from the cellulose source.



Site	LF	CB	VIF	Basel	Bern	Magadino	Payerne	Zurich	ANDRA-OPE
Classification	Urban Background	Urban centre	Peri-urban	Suburban	Urban-traffic	Rural	Rural	Urban	Rural background

Figure 4: Mean cellulose concentrations (ng m^{-3}) at each site, by season: spring (blue), summer (orange), autumn (grey) and winter (yellow). Black error bars represent one standard deviation of the seasonal averages. Only positive error bars are added, for clarity. **Note:** LF = Les Frênes; CB = Caserne de Bonne. Grenoble-based sites represented by CB, LF and Vif.

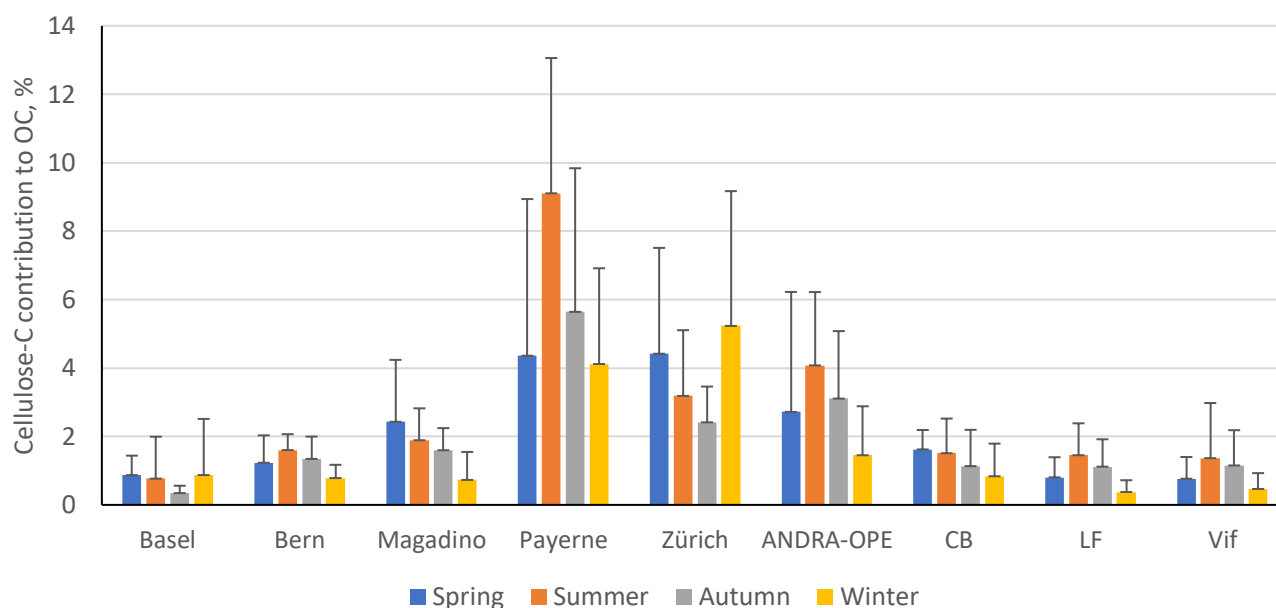
451 Whilst this is the general case, there are notable exceptions. Both the urban centres of Zurich
 452 and CB show very little seasonal variability compared to their more rural counterparts.
 453 Cellulose concentrations in Basel (suburban) also show minimal seasonality, but this may be
 454 due to concentrations being too small to exhibit a full seasonal pattern. This is surprising, given
 455 the close proximity of the site to a park-like area with trees and gardens. The lack of seasonality
 456 in urban settings, however, is consistent with the findings of Caseiro (2008). Additionally,
 457 Caseiro (2008) provided some evidence of cellulose concentrations at urban sites being greater
 458 than for nearby rural or background sites, with residential areas being an intermediate case.
 459 Within our Grenoble-based dataset as a comparison, CB (urban) does indeed exhibit cellulose
 460 concentrations marginally higher than the urban background site of LF and significantly higher
 461 than Vif (peri-urban).

462
 463 Alongside Basel, Caserne de Bonne also deviates from the general trend of summer-autumn
 464 maxima in cellulose concentrations observed across the other seven locations investigated here.
 465 Reasons for this are unclear, but this is suggestive of a source change in atmospheric plant
 466 debris, or an additional source being present at some urban locations, that may mask the typical
 467 seasonality. Given that these locations are urban in character, the weak seasonal variations may
 468 be owing to anthropogenic activity. This will be investigated in section 3.5.

469 3.4 Contribution of Cellulose-C to OC

470

471 To determine the overall importance of cellulose contribution to PM, the percentage
 472 contribution of cellulose-carbon to total organic carbon (Cellulose-C to OC) was determined.
 473 Figure 5 illustrates this seasonal average percentage contribution. Table S3 summarises
 474 numerically the overall average and seasonal percentage contributions and the ratio of
 475 cellulose-C contribution during winter and summer. Also highlighted is the maximum
 476 contribution of cellulose-C to OC experienced over the respective sampling periods at each
 477 site.



Site	LF	CB	VIF	Basel	Bern	Magadino	Payerne	Zurich	ANDRA-OPE
Classification	Urban Background	Urban centre	Peri-urban	Suburban	Urban-traffic	Rural	Rural	Urban	Rural background

Figure 5: Seasonal contributions of cellulose-C to OC (%) in PM₁₀ across the nine sites. Seasons are as follows: Spring (blue) - Mar-May; Summer (orange) - Jun-Aug; Autumn (grey) - Sep-Nov; Winter (yellow) - Dec-Feb. Black error bars represent one standard deviation of the mean values. Only positive error bars are included, for clarity. **Note:** LF = Les Frênes, CB = Caserne de Bonne. Grenoble-based sites represented by CB, LF and Vif.

478 The highest contributions to OC were typically found at rural sites, potentially due to fewer
 479 local sources of OC in rural sites compared to more urban locations. In fact, the annual
 480 contribution to OC found at Payerne (5.9 ± 4.4 %) is the highest found in literature. However,
 481 the annual average for the urban site of Zurich is also in a high range, at 3.8 ± 2.9 %. Regarding
 482 seasonal contributions, the rural sites in this study show a significantly different seasonal
 483 pattern compared those found in the study by Sánchez-Ochoa et al. (2007). Here, we see a
 484 noticeably smaller contribution of cellulose-C to OC during winter compared to summer. This

485 is reflected in the respective winter/summer ratios of cellulose-C contribution: the values in
486 this study range between 0.36 – 0.45, in comparison to 4.2 and 0.3 at the PM₁₀ rural and high-
487 altitude sites used in their study (Sánchez-Ochoa et al., 2007).

488

489 While seasonal contributions appear to be moderate in most cases, the contribution of cellulose-
490 C within episodes can be much more significant. It is also worth noting that these contributions
491 to OC are derived from free cellulose concentrations. Thus, the contribution to overall OC will
492 be higher when considering total cellulose. At sites with typically lower seasonal contributions
493 (Basel, Bern, LF), the episodic contributions reached between roughly 4.1 to 6.3 %. However,
494 at the sites that illustrated a much higher seasonal average contribution to OC, the maximum
495 contributions during episodes were found to be between 16.1 % at Zurich and 19.7 % at
496 Payerne. These maximum contributions (detailed in Table S3) are similar to those found at the
497 background sites by Sánchez-Ochoa et al. (2007). These values stand to highlight the
498 substantial contribution that atmospheric plant debris can have on atmospheric composition. In
499 other words, PBAP, and plant debris in particular, can contribute greatly to OM and must be
500 considered within all future characterisation and source apportionment studies.

501

502 Lastly, the contribution of coarse mode (PM with diameter less than 10 µm and greater than
503 2.5 µm) cellulose-C to coarse mode OC was evaluated at the three sites that completed both
504 PM₁₀ and PM_{2.5} analysis (ANDRA-OPE, Payerne and Zurich). This can be seen in Table S4,
505 in the SI. As PM_{2.5} data for ANDRA-OPE was only available for the 2020 sampling campaign,
506 PM₁₀ data from 2016 and 2017 was excluded. Table S4 shows a contribution of coarse
507 cellulose-C to be 3.16% at ANDRA-OPE, which is of very similar magnitude to that of the
508 overall cellulose-C contribution to OC. This is potentially due to the significant reduction in
509 cellulose source strength at the ANDRA-OPE site during the year of 2020, compared to the
510 years prior. This will be discussed in section 3.7. However, at both Payerne and Zurich, the
511 annual contributions to coarse OC are notably higher (11.02 % and 13.04 %, respectively) than
512 that of overall cellulose-C to OC (5.88 % and 3.76 %, respectively). From this data, we can see
513 that plant debris makes up a significant component of the coarse fraction of OM within these
514 two datasets.

515 3.5 Investigation of cellulose emission sources

516

517 To further evaluate the potential sources of plant debris into the atmosphere, correlations
 518 between cellulose and other source-specific tracers were investigated. This is the first cellulose
 519 field study to investigate these correlations with other tracers. Briefly, three specific sources
 520 have been hypothesised in the literature: direct biogenic emissions, unpyrolysed cellulose
 521 during domestic biomass burning, and anthropogenic resuspension and milling of plant debris
 522 (Sánchez-Ochoa et al., 2007; Caseiro, 2008; Yttri et al., 2011a; Yttri et al., 2011b). The
 523 chemical tracers used as proxies for these sources in this study are i) glucose and polyols, ii)
 524 levoglucosan, and iii) EC, Ca²⁺ and Ti, respectively. A suite of correlation coefficients
 525 (Spearman's rank correlation, *R_s*) was created for each site to monitor variations in correlations
 526 between site types using daily samples. Spearman's rank correlation was used in this section
 527 to better account for anomalous results between different datasets (e.g. cellulose vs polyols).
 528 A value of 1 indicates a perfect positive correlation, and a value of -1 indicates a perfect
 529 negative correlation. Table 5 shows the strength of the cellulose-tracer correlation at individual
 530 sites across the entire sampling period. A full table, inclusive with the number of data points
 531 (n) and p values for each correlation, plus *R_s* values within each season, can be found in the SI
 532 (Table S5).

*Table 5: Spearman correlations (*R_s*) between cellulose and characteristic chemical tracers across the nine sites. A red cell indicates a positive correlation between cellulose and the selected chemical tracer, whilst a blue cell indicates a negative correlation. A colour-coded key of corresponding *R_s* values is to the right of the table. Grenoble-based sites: CB – Caserne de Bonne, LF – Les Frênes and Vif. **Note: polyols = sum of arabitol, mannitol and sorbitol.***

<i>R_s</i>	CB	LF	Vif	Basel	Bern	Magadino	Payerne	Zurich	ANDRA-OPE	
Polyols	0.28	0.60	0.42	0.33	0.61	0.78	0.68	0.43	0.66	1.00
Glucose	0.28	0.57	0.48	0.39	0.63	0.66	0.71	0.43	0.58	0.66
Levoglucosan	-0.06	-0.38	-0.08	0.00	-0.07	-0.37	-0.18	-0.03	-0.43	0.33
EC	0.19	-0.08	0.04	0.34	0.25	-0.03	0.07	0.25	0.11	0.00
Ca ²⁺	0.14	0.28	0.12	0.37	0.45	-0.12	0.21	0.29	0.33	-0.33
Ti	0.28	0.34	0.03	0.40	0.39	0.05	0.31	0.31	0.18	-0.66
										-1.00

Site	LF	CB	VIF	Basel	Bern	Magadino	Payerne	Zurich	ANDRA-OPE
Classification	Urban Background	Urban centre	Peri- urban	Suburban	Urban- traffic	Rural	Rural	Urban	Rural background

533 Biogenic sources

534

535 The best understood chemical tracers for biogenic emissions are polyols (sum of arabitol,
 536 sorbitol and mannitol) and glucose (Bauer et al., 2008; Zhang et al., 2010; Després et al., 2012).

537 Glucose is the most abundant monosaccharide amongst vascular plants, is an important carbon
538 source for bacteria and fungi, and remains stable in the atmosphere (Jia et al., 2010; Zhu et al.,
539 2015). Its multiple biological sources into the atmosphere means that it can provide a good
540 insight as to whether atmospheric plant debris comes from a predominantly biogenic source.
541 Polyols are also used to provide tracer correlations with cellulose. These species are typically
542 used as markers of airborne fungi but have also been found to be present within leaves and
543 pollen (Medeiros, 2006).

544

545 As we can see in Table 5, relatively strong positive correlations arise between cellulose and
546 the two selected biogenic source tracers at most sites. The strongest correlations were seen at
547 rural locations (Magadino, Payerne and ANDRA-OPE, $p < 0.0001$). However, Bern and LF,
548 traffic-impacted and urban background sites respectively, also showed similar R_s magnitudes
549 to their rural counterparts ($p < 0.0001$). This indicates that similar factors promote the emission
550 of all of cellulose, polyols and glucose. The remaining four sites, all urban in character, showed
551 weaker correlations of cellulose with both glucose and polyols. It should also be said that
552 correlations across all sites were of similar magnitude when comparing cellulose-glucose and
553 cellulose-polyol concentrations. The stronger correlations at the rural sites indicate that a
554 significant portion of atmospheric cellulose, and thus plant debris, arises from biogenic sources
555 at these sites. As the values are typically below 0.7, this could suggest a different timing of
556 emissions between biogenic tracers and cellulose (e.g. meteorological conditions favouring
557 emission of fungal spores before plant debris). This is a distinct possibility, given that sampling
558 ranges between 3-6 days at the nine locations. Additionally, these moderate correlations with
559 biogenic tracers could be due to some input from other sources, but of a lower magnitude. By
560 contrast, the weaker correlations observed at most urban sites suggest that there remain other,
561 potentially more prominent, sources at play that determine atmospheric cellulose
562 concentrations. The two exceptions to this, LF and Bern, show that the sources of atmospheric
563 plant debris are not consistent within each designated site type.

564

565 It is noteworthy that the five locations that illustrate the strongest correlations with glucose and
566 polyols are the five out of the six sites in which the common, general-case seasonality is
567 observed. It is thus likely that this typical seasonality pattern is observed where the biogenic
568 source of plant debris is the most dominant.

569 **Biomass Burning**

570

571 A potential second source of atmospheric cellulose was proposed by Sánchez-Ochoa et al.
572 (2007) to account for anomalous high cellulose concentrations during winter. They suggested
573 that they were caused by unburned cellulose during biomass burning (Sánchez-Ochoa et al.,
574 2007). They also concluded that it was an unlikely process, based on the work of Schmidl et
575 al. (2005) illustrating that only a very small concentration of cellulose can be found in wood
576 smoke. Nevertheless, correlations between cellulose and levoglucosan, a chemical tracer for
577 biomass burning, were completed here to provide a more robust understanding of the viability
578 of this hypothesis (Giannoni et al., 2012; Madsen et al., 2018).

579

580 Table 5 indicates cellulose-levoglucosan tracers across all sites show no correlation with one
581 another, and in some instances show a moderate anti-correlation (R_s -0.43 – 0.00, p 0.0001 –
582 0.98). Stronger anti-correlations were seen at sites that also showed strong correlations with
583 biogenic tracers. Given that the theory was based on a winter-time source of atmospheric
584 cellulose via biomass burning, it is important to view the seasonal correlations to gain a fuller
585 understanding (Table S5, SI). Of all sites, the Grenoble-based locations (Caserne de Bonne,
586 Les Frênes and Vif) were the only three to have greater than the thirty data points of
587 simultaneous cellulose and levoglucosan measurements needed for a robust correlation. None
588 of these three locations showed any correlation between cellulose and levoglucosan (R_s 0.05 –
589 0.18, p 0.14 – 0.74). In fact, the remaining six locations showed also very weak correlation,
590 except for the site of Bern, which showed a moderate correlation (R_s 0.49, p < 0.03). But, as
591 already mentioned, the relatively small wintertime dataset for these six other sites (n = 21 to
592 25) does not provide strong confidence in these results. Thus, we can state that the sources of
593 atmospheric plant debris, as indicated by measurements of free cellulose, do not seem to
594 include any significant input from biomass burning from domestic wood. Further investigation
595 would be needed concerning possible emissions of total cellulose (included the one still
596 embedded in lignin).

597

598 **Other anthropogenic sources**

599

600 It has also been hypothesised that others anthropogenic activities may contribute to
601 atmospheric cellulose. Caseiro (2008) noticed typically higher cellulose concentrations in
602 urban locations, compared to the more rural ones within their study. The predominant

603 hypotheses for anthropogenic input of plant debris into the atmosphere were mechanisms such
604 as resuspension via road traffic, paper usage, and lawn mowing. To test these hypotheses,
605 correlations were computed between cellulose and known chemical tracers for man-made
606 emissions and mineral dust: Elemental Carbon (EC) and Ti/Ca^{2+} , respectively. EC is a known
607 primary product of combustion processes and is dominated by anthropogenic sources,
608 including road traffic, in urban areas (Wu and Yu, 2016). Ca^{2+} is also used as a tracer for
609 mineral dust, which commonly enters the atmosphere via road wear, gritting and dust
610 resuspension due to transport, as well as via gusts of wind (Denier van der Gon et al., 2010).
611 At the Swiss sites, Ca metal was measured as opposed to the soluble ion Ca^{2+} , but is still a
612 suitable tracer for mineral dust. Titanium metal is also used as a chemical tracer for mineral
613 dust and thus should possess a similar resuspension mechanism (Charron et al., 2019). A
614 positive correlation with these dust tracers would suggest plant debris is resuspended into the
615 atmosphere via the same established mechanism as mineral dust.

616

617 Considering EC first, Table 5 shows typically weak positive correlations between EC and
618 cellulose abundance at sites considered to be urban or traffic-impacted in character, excluding
619 Les Frênes (R_s 0.25 – 0.34, $p < 0.03$). The rural-based sites showed very little correlation (R_s
620 -0.03 – 0.11, p 0.16 – 0.79), suggesting that any resuspension mechanism of plant debris
621 involving automotive vehicles is only active in more built-up areas. In any case, automotive
622 resuspension of plant debris appears to be relatively weak, even when present at the more urban
623 locations.

624

625 In general, cellulose correlations with the two mineral dust chemical tracers were slightly
626 stronger across all sites compared to their respective cellulose-EC correlations. These values
627 were once again higher at more urban locations compared to rural sites, in particular at Basel
628 and Bern, which show R_s values between 0.37 and 0.45 ($p < 0.001$). The stronger correlations
629 with mineral dust do seem to suggest that ambient cellulose concentrations are somewhat
630 influenced by the resuspension of plant debris in a manner similar to that of mineral dust. Yet,
631 given the lack of significant correlation with EC, it seems that a resuspension mechanism may
632 not include a vehicular input. Other anthropogenic resuspension mechanisms not related to
633 traffic may contribute; paper usage (e.g. newspaper and cardboard production) has been
634 mooted in previous literature (Caseiro, 2008). These still unknown mechanisms could shadow
635 the seasonality of cellulose concentrations in more urban locations. One possible process
636 without anthropogenic input, however, could be via strong gusts of wind that resuspend this

637 plant material. Agricultural activities can also play a large role in emitting plant matter into the
638 atmosphere. Samaké et al. (2019b) showed maximum cellulose concentrations occurred during
639 harvest (summer) at ANDRA-OPE. This agricultural input from harvested land is also a major
640 emission source of polyols and glucose, which may explain the strong correlations of cellulose
641 with these tracers at the more rural locations (Samaké et al., 2019b). A lot of these processes
642 (seed emission, harvest, mowing, tree cutting, street sweeping and traffic etc.) are highly
643 sporadic and are subject to significant uncertainties, such as particle loads before, during and
644 after rain.

645

646 Overall, several conclusions can be drawn for the three potential sources proposed in the
647 literature. Firstly, the direct biogenic source of atmospheric plant debris is by far the most
648 significant, showing moderate to strong Spearman correlations between cellulose and other
649 characteristic biogenic tracers. This is particularly clear in rural sites; the correlation is
650 inconsistent among other site types. In addition, there is no source of atmospheric plant debris
651 that arises from biomass burning across any season or site type, as already suggested by Borlaza
652 et al. (2021a). Lastly, the resuspension of plant material could be another possible input to
653 overall ambient plant debris abundance. This mechanism does not seem to incorporate road
654 traffic in the way suggested by Caseiro (2008), given the lack of correlation between cellulose
655 and EC abundance.

656

657 **3.6 Local vs. regional origin**

658

659 Seasonal cellulose variations do not show a similar pattern across all sites, nor one that is
660 consistent across different regions and scales. This trend, or lack thereof, was expressed
661 numerically using correlation coefficients (R^2) of monthly concentration averages for the
662 groups of sites that were sampled at the same time. As shown in Table 6, the correlations
663 between sites within the Grenoble metropole (CB, LF and Vif) are low to moderate. This is
664 also the case for the Swiss sites, which span a much larger spatial range compared to the
665 Grenoble-based sites. The lack of a shared temporal variability seems to indicate that the major
666 sources of plant debris are most likely to be local to each site. It may also suggest that several
667 mechanisms impacting ambient cellulose concentrations contribute to different degrees
668 according to the investigated site (Caseiro, 2008; Winiwarter et al., 2009; Borlaza et al., 2021).
669 Moderate correlations between the traffic-impacted location in Bern with the two rural sites of
670 Magadino and Payerne were the highest among the Swiss sites. Regardless, these values are

671 not indicative of a common source. The Grenoble-based sites of LF and Vif do seem to show
 672 a slight exception, producing an R^2 value close to 0.7 ($p < 0.0001$). The three monitoring
 673 locations within the Grenoble metropole are within 15 km of one another, so a common source
 674 of atmospheric plant debris on local scales of this magnitude remains possible.

Table 6: Correlations (R^2) monthly cellulose concentrations between the Swiss sites (top) and between Grenoble-based (bottom) sites (LF, CB and Vif). The colour-coded key (right) gives the corresponding colour of the correlation strength (R^2 values). A strong correlation (R^2 close to 1) is coded red, with no correlation coded blue. Intermediate correlations are coded white. Note: CB = Caserne de Bonne, LF = Les Frênes. Grenoble-based sites represented by CB, LF and Vif.

R^2										
Bern	0.0092									
Magadino	0.0059	0.4636								1
Payerne	0.016	0.4275	0.2941							0.8
Zurich	0.0124	0.395	0.1814	0.0046						0.6
	Basel	Bern	Magadino	Payerne						0.5
										0.4
										0.2
										0

R^2		
CB	0.0056	
VIF	0.6944	0.0172
	LF	CB

Site	LF	CB	VIF	Basel	Bern	Magadino	Payerne	Zurich
Classification	Urban Background	Urban centre	Peri-urban	Suburban	Urban-traffic	Rural	Rural	Urban

675
676
677
678
679

680 The R^2 values in Table 6 were compared to correlations between monthly mean concentrations
 681 of the so-called polyol fraction (i.e., sum of arabitol, mannitol and sorbitol) for the same set of
 682 locations (Samaké et al., 2019a; Borlaza et al., 2021a; Grange et al., 2021). In contrast to
 683 cellulose, polyols show common temporal variations, with R^2 correlations ranging from 0.4 –
 684 0.91 and 0.95 – 0.98 ($p < 0.0001$) within the groups of Swiss and Grenoble-based sites,
 685 respectively (Table S6 and Table S7). Polyols are used as chemical tracers for fungal spores, a
 686 very common class of PBAP, and here provide a near perfect example of a PBAP class
 687 displaying homogenized concentration variations over time at a regional scale. This suggests a
 688 single common source of polyols that is impacted similarly by external factors across all
 689 locations, especially at short range e.g. within the Grenoble area. This was also suggested by
 690 Borlaza et al. (2021) during their PMF study, and by Samaké et al. (2019a) as part of their
 691 study across all of France. Moreover, Samaké et al. (2020, 2021) evidenced that the presence

692 of fungi and bacteria in ambient air is mostly related to a limited number of microorganism
693 species only, which vary from one climatic region to the next.

694

695 The stark contrast between the two sets of chemical tracers (cellulose vs. polyols) highlights
696 the rather local nature of atmospheric plant debris and its sources. Given that meteorology is
697 relatively consistent on a short to medium scale (< 200 km), it would be expected that plant
698 debris emissions would impact all sites of a given area similarly. However, heterogeneous
699 distribution of the diverse plant species at the city (or regional) scale might induce specific
700 temporal variations in the emissions of plant debris at the local scale. Therefore, the lack of
701 correlation in cellulose datasets may result from site-to-site differences in the dominant sources
702 (flora) or emission processes of ambient plant debris (Caseiro, 2008).

703

704 **3.7 Interannual Comparison – A Combined Approach**

705

706 Cellulose concentrations were measured over two separate time periods: 2017-18 and 2020-21
707 in Grenoble, and over three separate time periods: 2016, 2017 and 2020 at ANDRA-OPE.
708 These multiple datasets (with a similar number of data points) gave us the opportunity to assess
709 the interannual variations of atmospheric plant debris, in the same regions. This provided the
710 possibility to combine the various analyses used in the above sections as part of a more small-
711 scale, holistic investigation.

712 **Grenoble**

713 Figure 6 presents the seasonal mean cellulose concentrations across the two time periods within
714 the Grenoble metropole (expressed numerically in Table S8, SI). The difference in cellulose
715 concentrations between different sampling years is stark. Both CB and Vif show significant
716 decreases in cellulose concentrations from 2017-18 to 2020-21, with the exception of the spring
717 period. For example, summer and autumn cellulose concentrations decreased by over a factor
718 of 3 between 2017-18 and 2020-21. This is not the case for the urban background site of Les
719 Frênes, where the seasonal concentrations typically increased across all seasons except for
720 spring.

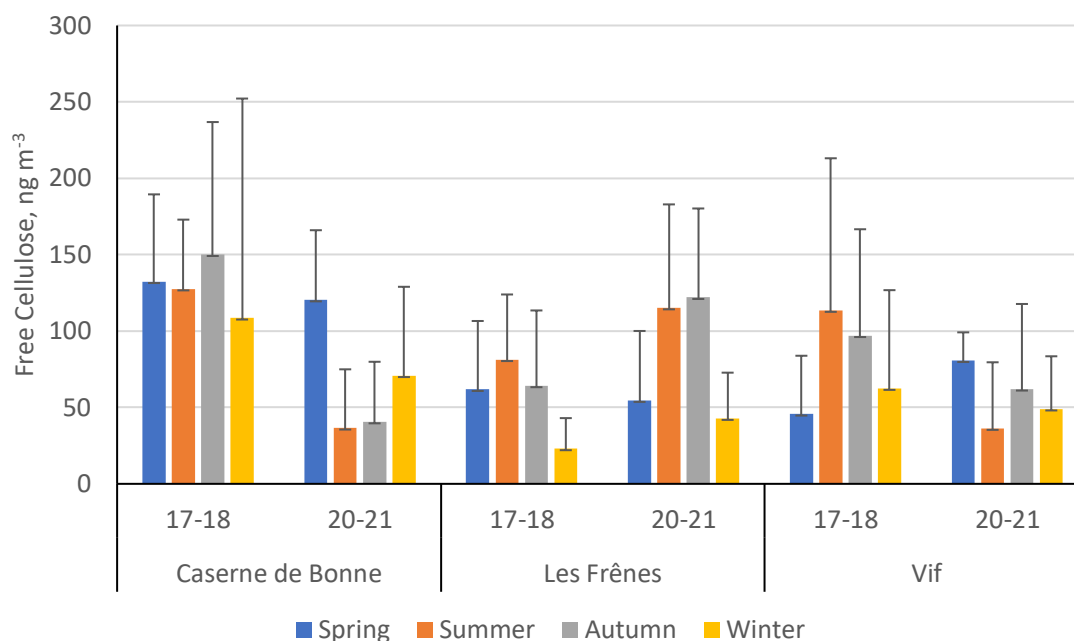


Figure 6: Seasonal mean averages of cellulose concentrations (ng m^{-3}) of the three sites within the Grenoble metropole across the two separate sampling periods: 2017-18 and 2020-21. Black error bars represent one standard deviation of the seasonal means. Only positive error bars are shown to aid clarity. Seasons are defined as: Dec-Feb (winter), Mar-May (spring), Jun-Aug (summer), Sep-Nov (autumn). Site classifications are as follows: Caserne de Bonne – urban; Les Frênes – urban background; Vif – peri-urban.

721 Temperature data was used as an attempt to elucidate the contrasting concentrations across the
 722 two sampling periods (Fig. S4, SI). A warmer and more humid climate brings about greater
 723 biological activity (e.g. an increase in pollen production), but can also speed up the
 724 decomposition processes involved in generating plant debris (Liu et al., 2006; Martínez et al.,
 725 2014; Verma et al., 2018). Temperature data for Grenoble across the two sampling periods was
 726 provided by Atmo Auvergne-Rhône-Alpes (Atmo AURA).

727
 728 Seasonal and monthly average temperatures across the two sampling periods show some
 729 differences, but the variation is slight (Fig. S4, SI). It is highly unlikely in this instance that the
 730 large variations in the atmospheric cellulose concentrations were caused by ambient
 731 temperature changes. This is further supported by the lack of change in seasonal average polyol
 732 concentrations for the same sites, shown in Fig. S5, whose concentrations are impacted solely
 733 by biogenic factors (Bauer et al., 2008; Zhang et al., 2010; Després et al., 2012). While other
 734 climate data were not been available, there is potential for the variability in cellulose source
 735 strengths to have been caused by factors that are not purely meteorological. This observed
 736 variability may be related to changes in human activities, associated with the COVID-19

737 lockdown and sanitary restrictions. This would most profoundly affect the pedestrianised urban
 738 centre of Caserne de Bonne, with the prolonged closure of shops in the area surrounding the
 739 sampling site, together with the decrease of traffic on the nearby avenues.

740

741 Interestingly, changes in ambient cellulose concentrations across the two periods are
 742 concomitant with changes in the contribution of cellulose-C to OC (Fig. 7, numerical values
 743 Table S9). Thus, it is likely that changes in atmospheric cellulose concentrations will have
 744 resulted from changes in the source strength of plant debris, and not from a wider-scale
 745 reduction in some or all other OC sources.

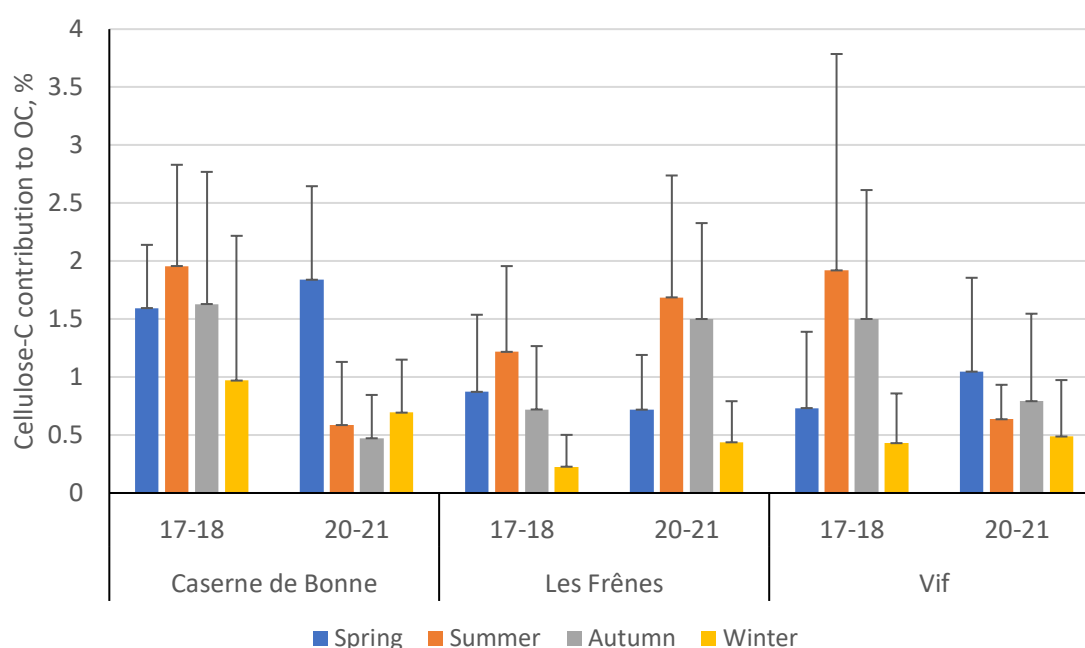


Figure 7: Percentage contribution of cellulose-derived carbon towards overall organic carbon (cellulose-C to OC) across the three sites within the Grenoble metropole during the two separate sampling periods: 2017-18 and 2020-21. Black error bars represent one standard deviation of the seasonal means. Only positive error bars are shown to aid clarity. Seasons are defined as: Dec-Feb (winter), Mar-May (spring), Jun-Aug (summer), Sep-Nov (autumn).

Site classifications are as follows: Caserne de Bonne – urban; Les Frênes – urban background; Vif – peri-urban.

746 Given that these large interannual variations seemed to be predominantly limited to cellulose
 747 and not the remaining sources of OC, it was necessary to evaluate the potential sources once
 748 more. Following section 3.5, cellulose-tracer correlations were again produced using the same
 749 characteristic source tracers for the two periods, to see if changes in cellulose concentrations
 750 were consistent with variations in tracer correlations. These correlation coefficients can be seen
 751 in Table 7 (Table S10 for full table). From the two sets of correlations, it is evident that the

752 sources of plant debris are only consistent between campaigns at Les Frênes. Reasonable
 753 correlations with characteristic biogenic chemical tracers (polyols and glucose) remain
 754 consistent, whilst a moderate anti-correlation is still seen between cellulose and levoglucosan.
 755 No correlations with EC were seen throughout the two campaigns.

Table 7: Spearman correlations (R_s) between cellulose and characteristic chemical tracers at the Grenoble-based sites, across the two separate sampling periods: 2017-18; 2020-21. A red cell indicates a positive correlation between cellulose and the selected chemical tracer, whilst a blue cell indicates a negative correlation. A colour-coded key of corresponding R_s values is to the right of the table.

Site classifications are as follows: Caserne de Bonne (CB) – urban; Les Frênes (LF) – urban background; Vif – peri-urban. **Note: polyols = sum of arabitol, mannitol and sorbitol.**

Rs	Grenoble 2017 - 2018			Grenoble 2020 - 2021			
	CB	LF	Vif	CB	LF	Vif	
							1.00
							0.66
Polyols	0.46	0.63	0.59	-0.09	0.68	0.22	0.33
Glucose	0.47	0.62	0.66	-0.08	0.56	0.24	0.00
Levoglucosan	-0.07	-0.48	-0.21	0.25	-0.38	0.10	-0.33
EC	0.15	-0.11	-0.07	0.18	0.01	0.16	-0.66
Ca ²⁺	0.14	0.22	0.00	0.31	0.32	0.32	-1.00

756 By contrast, tracer correlations across both CB and Vif vary significantly between the two
 757 campaigns. R_s values of cellulose versus glucose or polyol concentrations decrease
 758 significantly during the 20/21 campaign. A weak positive correlation becomes apparent
 759 between cellulose and Ca²⁺ concentrations during the 20/21 campaign that was absent during
 760 the previous series. This is particularly visible at Vif, but it is also a consistent trend across all
 761 three sites. These findings suggest potentially two possible hypotheses. Firstly, the contribution
 762 of plant debris arising from biogenic sources has been much weaker during the second
 763 campaign at CB and Vif, compared to three years earlier, thus showing little to no correlation
 764 with characteristic biogenic tracers. This may be the reason for the weakened seasonality at
 765 both CB and Vif. Secondly, the increased correlation with Ca²⁺ during 20/21 implies a better
 766 correlation between plant debris and mineral dust abundance. This in turn could suggest a slight
 767 increase in the strength of plant matter resuspension during the second campaign, compared to
 768 2018-19.

769 **ANDRA-OPE**

770 Figure 8 shows the seasonal mean average free cellulose concentrations (ng m^{-3}) for three
 771 separate sampling campaigns (2016, 2017 and 2020) at ANDRA-OPE (numerical values in
 772 Table S11, SI). During the 2017 monitoring campaign, an extended period of sampling was
 773 completed with samples being taken on average 5 times per week during summer. For this
 774 interannual analysis, it was important to bring the number of data points in line with the datasets
 775 from 2016 and 2020. Samples were removed from the 2017 dataset until the same sampling
 776 frequency was obtained across all the periods (1 sample taken every sixth day). As can be seen
 777 in Fig. 8, cellulose concentrations dropped significantly between 2016/2017 and 2020, with the
 778 exception of the winter period. This is in a manner very similar to the variations seen at the CB
 779 and Vif sampling sites from within the Grenoble metropole. The data for the winter period in

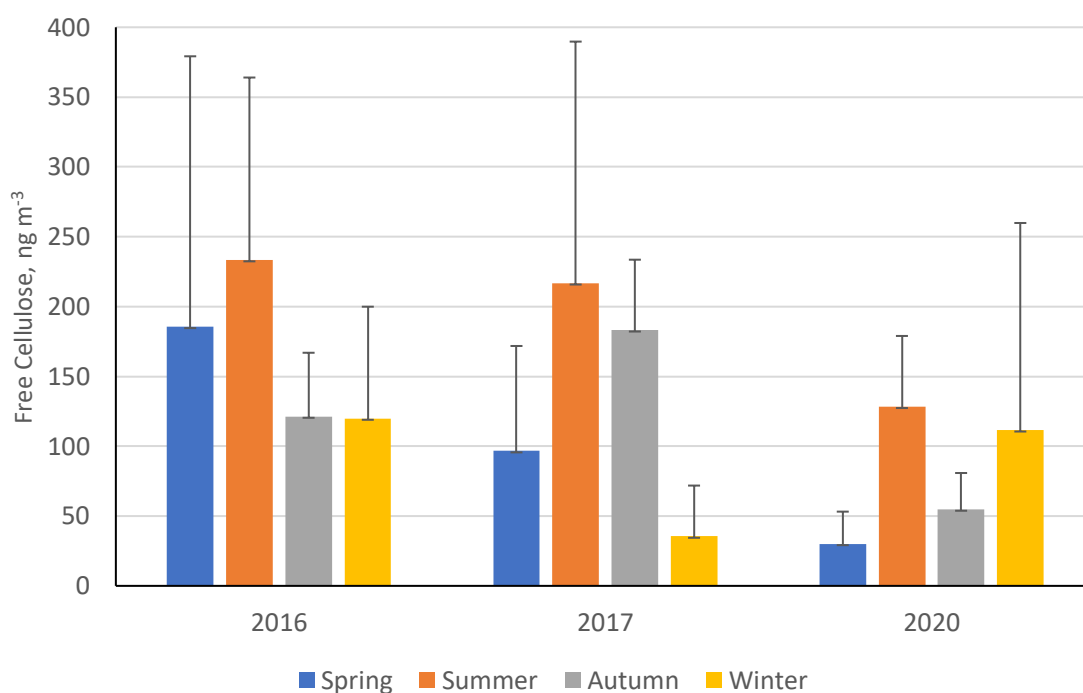


Figure 8: Seasonal mean averages of cellulose concentrations (ng m^{-3}) at ANDRA-OPE (rural site) during the three separate sampling periods: 2016, 2017 and 2020. Black error bars represent one standard deviation of the seasonal means. Only positive error bars are shown to aid clarity. Seasons are defined as: Dec-Feb (winter), Mar-May (spring), Jun-Aug (summer), Sep-Nov (autumn).

780 2020 comes predominantly from before the COVID-19 pandemic, so it is possible for the
 781 significant reduction in anthropogenic activities being a major factor in the reduction of
 782 atmospheric cellulose concentrations. However, it should be mentioned that agricultural

783 activities (fertilisation, harvest, ploughing, etc...) were not affected by the COVID-19
784 associated restrictions.

785 Further, we once again see a noticeable reduction in the contribution of cellulose-C to OC (%)
786 during the 2020 sampling period, compared to the two previous campaigns, especially during
787 summer and autumn (Fig. 9, numerical values Table S12, SI). This suggests that the source of
788 atmospheric plant debris became significantly weaker during 2020, when placed in the context
789 of overall OC atmospheric emission. Unlike the Grenoble metropole dataset, at ANDRA-OPE
790 the seasonal variations of cellulose concentrations and the respective contributions of cellulose-
791 C to overall OC are different. This may suggest that other emission sources of OC have varied
792 at ANDRA-OPE, compared to the more consistent OC emission within Grenoble across its
793 sampling periods.

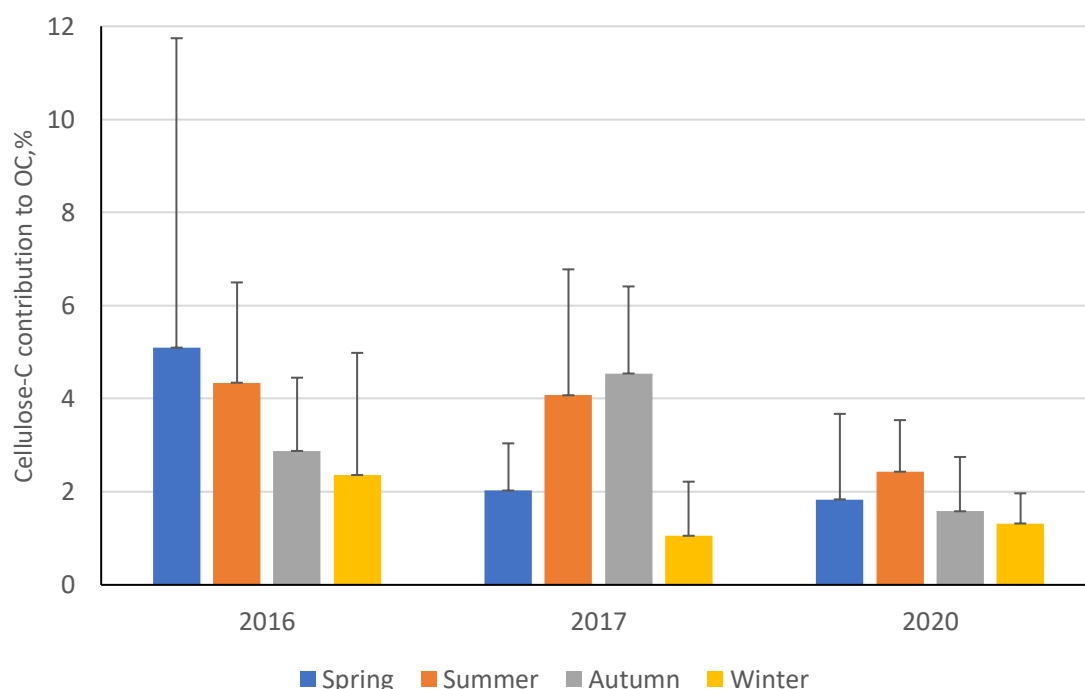


Figure 9: Percentage contribution of cellulose-carbon towards overall organic carbon (cellulose-C to OC) at ANDRA-OPE during the three separate sampling periods: 2016, 2017 and 2020. Black error bars represent one standard deviation of the seasonal means. Only positive error bars are shown to aid clarity. Seasons are defined as: Dec-Feb (winter), Mar-May (spring), Jun-Aug (summer), Sep-Nov (autumn).

794 Following these significant interannual variations within cellulose concentrations and
795 cellulose-C to OC, correlations of cellulose with source-specific tracers were completed to see
796 how the source of atmospheric plant debris has changes between the three sampling periods
797 (Table 8, p values in Table S13, SI). The three sampling periods at ANDRA-OPE exhibit
798 significant variations in their cellulose-tracer correlations. Notably, the correlations of
799 cellulose with biogenic tracers (polyols and glucose) remain generally moderate throughout,

800 and in fact are weakest during the 2016 campaign. This suggests that, at the rural site of
 801 ANDRA-OPE, the significant reduction in atmospheric cellulose concentrations during 2020
 802 is consistent with that of the changes within other biogenic chemical tracers. Further, during
 803 the 2020 campaign, a relatively strong correlation is seen between cellulose and Ca^{2+} , a mineral
 804 dust tracer, that is absent during the previous two campaigns. This potentially implies a
 805 significant contribution to cellulose concentrations from an anthropogenic source, or reflects a
 806 correlation to wind speed. An anthropogenic source would be unlikely however, given the rural
 807 nature of this sampling site and its lack of proximity to anthropogenic inputs, outside of
 808 agriculture.

*Table 8: Spearman correlations (R_s) between cellulose and characteristic chemical tracers at ANDRA-OPE, across the three separate sampling periods: 2016, 2017 and 2020. A red cell indicates a positive correlation between cellulose and the selected chemical tracer, whilst a blue cell indicates a negative correlation. A colour-coded key of corresponding R_s values is to the right of the table. **Note: polyols = sum of arabitol, mannitol and sorbitol.***

R_s	ANDRA-OPE			
	2016	2017	2020	
Polyols	0.44	0.52	0.63	1.00
Glucose	0.21	0.57	0.41	0.66
Levoglucosan	-0.31	-0.30	-0.68	0.33
EC	-0.12	0.03	0.08	0.00
Ca^{2+}	0.23	0.11	0.62	-0.33
				-0.66
				-1.00

809 Overall, these results at ANDRA-OPE and within the Grenoble conurbation indicate for the
 810 first time a large interannual variability in the sources and drivers of atmospheric cellulose, and
 811 highlight our emerging knowledge of these processes.

812

813 4. Conclusions

814

815 Previous work has acknowledged the potential contribution of atmospheric cellulose to PM_{10}
 816 and atmospheric OC (Yttri et al., 2011b; Bozzetti et al., 2016; Borlaza et al., 2021). Yet, long-
 817 term studies using cellulose as a chemical tracer for atmospheric plant debris are still rare, and
 818 typically cover only few ambient conditions (Sánchez-Ochoa et al., 2007; Caseiro, 2008; Yttri
 819 et al., 2011a; Yttri et al., 2011b; Alves, 2017). Thus, an investigation of ambient cellulose
 820 concentrations, across a wide range of locations and site types, using a sensitive HPLC-PAD
 821 analysis and an improved hydrolysis method was undertaken. To date, with more than 1500

822 samples analysed in the exact same way, this is one of the most in-depth study of atmospheric
823 cellulose, its seasonality, spatiotemporal variability and its sources.

824

825 Annual mean free cellulose concentrations were found to range between $29 \pm 38 \text{ ng m}^{-3}$ at
826 Basel to $284 \pm 225 \text{ ng m}^{-3}$ at Payerne (suburban and rural sites, respectively). All rural sites and
827 half of the urban sites showed cellulose concentrations that were highest during summer and
828 autumn, coinciding with typically higher seasonal temperatures. This seasonality differs from
829 the spring-summer maximum illustrated by Sánchez-Ochoa et al. (2007). The remaining urban
830 sites deviated significantly from this pattern, showing no evidence of seasonal cellulose
831 variations. This suggests that different sources or processes may shadow the cellulose
832 seasonality in some urban areas. Cellulose concentrations generally correlated poorly between
833 sites, which implies a source of atmospheric plant debris that is highly localised.

834

835 For the first time, correlations of cellulose with chemical tracers, that are characteristic of
836 specific emissions sources, were completed to best apportion the origins of atmospheric plant
837 debris. It was shown that plant debris arises predominantly via direct biogenic emissions,
838 particularly at rural locations. Further, the sites showing the strongest correlations with
839 biogenic tracers were the same sites that exhibited the general summer-autumn cellulose
840 maxima. A potential secondary influence towards ambient cellulose concentrations comes via
841 resuspension of previously settled plant matter, comparable to that of mineral dust. The
842 mechanism associated with this source is unknown but is unlikely to possess a traffic signature
843 at the sites investigated, given the poor cellulose correlations with EC, a known tracer for
844 anthropogenic combustion mainly related to traffic in urban areas. This may be the factor that
845 masks seasonality at some urban sites. At rural locations, agricultural activities can be a
846 significant source of cellulose into the atmosphere during harvest, as demonstrated by Samaké
847 et al. (2019b). Lastly, biomass burning is not a source of atmospheric cellulose for the sites
848 investigated here.

849

850 The annual contribution of free cellulose-derived carbon to total organic carbon ranged
851 between 0.7 and 5.9 % for the measured locations, with rural sites typically showing higher
852 contributions. It should be noted that the percentage contribution of total cellulose-derived
853 carbon to OC would be greater than the above values. While the annual mean contributions to
854 OC seem moderate, this percentage can greatly increase during episodic cellulose
855 concentration spikes. The maximum percentage contributions seen of cellulose-C to OC at

856 Payerne and ANDRA-OPE were 19.7 and 18.3% respectively, which are consistent with other
857 background sites results found in the literature. These significant episodic contributions show
858 that cellulose and plant debris can play a significant role in the atmospheric composition.

859

860 The interannual variations of the cellulose concentrations at the same locations within the
861 Grenoble metropole were then assessed. Interestingly, the cellulose concentrations and the
862 contribution (%) of cellulose-C to OC showed significant fluctuations across the two periods
863 considered. The correlations of cellulose with other chemical tracers also vary significantly.
864 Reasons behind these dramatic fluctuations are not fully understood and this highlights our
865 limited knowledge of these atmospheric processes. Reduced human activities due to the
866 COVID-19 pandemic may be a factor. Further interannual studies must be undertaken to see if
867 these variations are a common occurrence, or unique to this dataset.

868

869 Given the local-scale source of atmospheric plant debris, more monitoring campaigns similar
870 to the one in the Grenoble metropole should be performed. An increase in sampling site
871 numbers, with varying micro-climatic and PM emission source characteristics, within a given
872 area should lead to a more concrete understanding of the spatial variability of plant debris. It
873 would open the road for the inclusion of cellulose into chemical transport models, in order to
874 better represent this component of the organic matter in PM, particularly important in rural
875 areas.

876

877 **Data availability:** All relevant data for this paper are archived at the IGE (Institut des
878 Géosciences de l'Environnement), and availability can be discussed with the corresponding
879 authors (Jean-Luc Jaffrezo).

880

881 **Acknowledgements:** The authors acknowledge the work of the many engineers in the lab at
882 IGE for the analyses (C. Voiron, R. Elazzouzi, B. Morisset, C. Le Bigaignon, J. Chazelle, A.
883 Vella, G. Fonkoh) as well as the dedicated efforts of many people at the sampling sites for
884 collecting the samples. A. M. Brighty would also like to thank S. Weber for his help and
885 guidance throughout the project. Samples from the 3 Grenoble sites were collected and
886 analysed within the program QAMECS (ADEME 1662C0029), coupled with funding from the
887 CARA program from LCSQA for the “Les Frênes” site.

888

889 The authors would like to thank all 3 referees for insightful comments that helped improving
890 the paper. Particularly, Pr Hans Puxbaum provided a long, precise, and detail text with account
891 of the historical aspects of past research on cellulose measurements in atmospheric PM, which
892 is extremely interesting and complete. His comments are now partially reflected in our paper,
893 but the original texts (RC1 and RC4) should be referred to, in order to give him full credit on
894 this point.

896 **Author contributions:** AMB performed all cellulose analyses, processed the data and wrote
897 up the manuscript. JLJ was the supervisor for the Masters of AMB. He directed all the
898 personnel who performed the analysis at IGE and designed the study. VJ designed the protocol
899 for cellulose analyses. JLJ and GU were the coordinators of the atmospheric part of the
900 Mobil'Air program in Grenoble; LJB was the curator of the atmospheric Mobil'Air data. SB
901 is the coordinator of the ANDRA-OPE site and atmospheric program, and provided the samples
902 from this site. CH is the head of the NABEL network in Switzerland, provided all samples
903 from this country and directed the program for this yearly sampling; SKG was the curator of
904 the swiss data. OF is responsible for the CARA program from the LCSQA in France, and
905 provided partial funding for sample analysis at LF site. CT was responsible for the sampling
906 by Atmo-AURA at the 3 sites in the Grenoble area. All authors reviewed and commented on
907 the manuscript.

908 **Competing interests:** The authors declare that they have no conflict of interest.

909 **References**

910 Alfarra, M. R., Prevot, A. S. H., Szidat, S., Sandradewi, J., Weimer, S., Lanz, V. A., Schreiber,
911 D., Mohr, M., and Baltensperger, U.: Identification of the mass spectral signature of organic
912 aerosols from wood burning emissions, *Environ. Sci. Technol.*, 41, 5770-5777, 2007.

913 Alleman, L. Y., Lamaison, L., Perdrix, E., Robache, A. and Galloo, J.-C.: PM10 metal
914 concentrations and source identification using positive matrix factorization and wind sectoring
915 in a French industrial zone, *Atmospheric Research*, 96(4), 612–625,
916 <https://doi.org/10.1016/j.atmosres.2010.02.008>, 2010.

917
918 Alves, C. A.: A short review on atmospheric cellulose, *Air Qual. Atmos. Health*, 10, 669–678,
919 2017.

920 Atmo AURA: <https://www.atmo-auvergnerhonealpes.fr/>, last access: 12 April 2021.

921 Aymoz, G., Jaffrezo, J. L., Chapuis, D., Cozic, J., and Maenhaut, W.: Seasonal variation of PM
922 10 main constituents in two valleys of the French Alps. I: EC/OC fractions, *Atmos. Chem.*
923 *Phys.*, 7(3), 661–675, 2007.

924 Bauer, H., Claeys, M., Vermeylen, R., Schueller, E., Weinke, G., Berger, A., and Puxbaum,
925 H.: Arabitol and mannitol as tracers for the quantification of airborne fungal spores, *Atmos.*
926 *Environ.*, 42(3), 588–593, 2008a.

927 Birch, M. E. and Cary, R. A.: Elemental carbon-based method for monitoring occupational
928 exposures to particulate diesel exhaust, *Aerosol Sci. Technol.*, 25(3), 221–241, 1996.

929 Borlaza, L. J. S., Weber, S., Uzu, G., Jacob, V., Cañete, T., Micallef, S., Trébuchon, C., Slama,
930 R., Favez, O., Jaffrezo, J., L.: Disparities in particulate matter (PM10) origins and oxidative
931 potential at a city-scale (Grenoble, France) - Part I: Source apportionment at three neighbouring
932 sites, *Atmos. Chem. Phys.*, 21(7), 5415–5437, 2021a.

- 933 Borlaza, L. J. S., Weber, S., Jaffrezo, J. L., Houdier, S., Slama, R., Rieux, C., Albinet, A.,
934 Micallet, S., Trébuchon, C., and Uzu, G.: Disparities in PM₁₀ origins and oxidative potential at
935 a city-scale (Grenoble, France) - Part II: Sources of PM₁₀ oxidative potential using multiple
936 linear regression analysis and the predictive applicability of multilayer perceptron neural
937 network analysis, *Atmos. Chem. Phys.*, 21(12), 9719–9739, [https://doi.org/10.5194/acp-21-](https://doi.org/10.5194/acp-21-9719-2021)
938 9719-2021, 2021b.
- 939 Borlaza, L. J. S., Weber, S., Marsal, A., Uzu, G., Jacob, V., Besombes, J. L., Conil, S., and
940 Jaffrezo, J. L.: Long-term trends of PM₁₀ sources and oxidative potential in a rural site in
941 France. Submitted to *Atmos. Chem. Phys. Disc.*, on 18/10/2021, 2021c.
- 942 Boucher, O., Randall, D., Artaxo, P., Bretherton, C., Feingold, G., Forster, P., Kerminen, V.-
943 M., Kondo, Y., Liao, H., and Lohmann, U.: Clouds and aerosols, in *Climate change 2013: the*
944 *physical science basis. Contribution of Working Group I to the Fifth Assessment Report of the*
945 *Intergovernmental Panel on Climate Change*, pp. 571– 657, Cambridge University Press.,
946 2013.
- 947 Bozzetti, C., Daellenbach, K. R., Heuglin, C., Fermo, P., Sciare, J., Kasper-Giebl, A., Mazar,
948 Y., Abbaszade, G., El Kazzi, M., Gonzalez, R., Shuster-Meiseles, T., Flasch, M., Wolf, R.,
949 Kreplová, A., Canonaco, F., Schnelle-Kreis, J., Slowik, J. G., Zimmermann, R., Rudich, Y.,
950 Baltensperger, U., El Haddad, I., and Prévôt, A. S. H.: Size-Resolved Identification,
951 Characterisation, and Quantification of Primary Biological Organic Aerosol at a European
952 Rural Site, *Environ. Sci. Technol.*, 50, 3425 – 3434, 2016.
- 953 Caseiro, A. F. F.: *Composição Química do Aerossol Europeu.*, PhD Thesis, Universidade de
954 Aveiro, Aveiro. [online] Available from: <https://core.ac.uk/download/pdf/15560924.pdf>
955 (Accessed 27 October 2020), 2008.
- 956 Cavalli, F., Viana, M., Yttri, K. E., Genberg, J., and Putaud, J.-P.: Toward a standardised
957 thermal-optical protocol for measuring atmospheric organic and elemental carbon: the
958 EUSAAR protocol, *Atmos. Meas. Tech.*, 3(1), 79–89, 2010.
- 959 Charron, A., Polo-Rehn, L., Besombes, J. L., Golly, B., Buisson, C., Chanut, H., Marchand,
960 N., Guillaud, G., and Jaffrezo, J. L.: Identification and quantification of particulate tracers of
961 exhaust and non-exhaust vehicle emissions for source apportionment studies, *Atmos. Chem.*
962 *Phys.*, 19(7), 5187–5207, <https://doi.org/10.5194/acp-19-5187-2019>, 2019.
- 963 Chevrier, F.: *Chauffage au bois et qualité de l'air en Vallée de l'Arve : définition d'un système*
964 *de surveillance et impact d'une politique de rénovation du parc des appareils anciens.*, PhD
965 Thesis, Université Grenoble Alpes, Grenoble. [online] Available from: [https://tel.archives-](https://tel.archives-ouvertes.fr/tel-01527559)
966 [ouvertes.fr/tel-01527559](https://tel.archives-ouvertes.fr/tel-01527559) (Accessed 5 January 2021), 2016.
- 967 Denier van der Gon, H., Jozwicka, M., Hendriks, E., Gondwe, M., and Schaap, M.: *Mineral*
968 *Dust as a component of Particulate Matters*, BOP Reports, The Netherlands, 2010.
- 969 Després, V. R., Alex Huffman, J., Burrows, S. M., Hoose, C., Safatov, A. S., Buryak, G.,
970 Fröhlich-Nowoisky, J., Elbert, W., Andreae, M. O., Pöschl, U., and Jaenicke, R.: Primary

- 971 biological aerosol particles in the atmosphere: a review, *Tellus B: Chemical and Physical*
972 *Meteorology*, 64, 15598, 2012.
- 973 Franke, V., Zieger, P., Wideqvist, U., Acosta Navarro, J. C., Leck, C., Tunved, P., Rosati, B.,
974 Gysel, M., Salter, M. E., and Ström, J.: Chemical composition and source analysis of
975 carbonaceous aerosol particles at a mountaintop site in central Sweden, *Tellus B Chem. Phys.*
976 *Meteorol.*, 69(1), 1353387, <https://doi.org/10.1080/16000889.2017.1353387>, 2017.
- f
- 977 Gelencsér, A., May, B., Simpson, D., Sánchez-Ochoa, A., Kasper-Giebl, A., Puxbaum, H.,
978 Caseiro, A., Pio, C. and Legrand, M.: Source apportionment of PM_{2.5} organic aerosol over
979 Europe: Primary/secondary, natural/anthropogenic, and fossil/biogenic origin, *J. Geophys.*
980 *Res.*, 112(D23), D23S04, <https://doi.org/10.1029/2006JD008094>, 2007.
- 981 Gelencsér, A.: *Carbonaceous Aerosol*, 1st edn, Springer, The Netherlands, 350 pages, 2004.
- 982 Giannoni, M., Martellini, T., Del Bubba, M., Gambaro, A., Zangrando, R., Chiari, M., Lepri,
983 L., and Cincinelli, A.: The use of levoglucosan for tracing biomass burning in PM_{2.5} samples in
984 Tuscany (Italy), *Environmental Pollution*, 167, 7–15, 2012.
- 985 Golly, B., Waked, A., Weber, S., Samaké, A., Jacob, V., Conil, S., Rangonio, J., Chrétien, E.,
986 Vagnot, M. P., Robic, P. Y., Besombes, J. L., and Jaffrezo, J. L.: Organic Markers And OC
987 Source Apportionment For Seasonal Variations Of PM_{2.5} At 5 Rural Sites In France, *Atmos.*
988 *Environ.*, 198, 142-157, <https://doi.org/10.1016/J.Atmosenv.2018.10.027>, 2019.
- 989 Gould, M. J.: Alkaline peroxide delignification of agricultural residues to enhance enzymatic
990 saccharification, *Biotechnol. Bioengng*, 26, 46–52, 1984.
- 991 Graham, B., Guyon, P., Taylor, P. E., Artaxo, P., Maenhaut, W., Glovsky, M. M., Flagan, R.
992 C., and Andreae, M. O.: Organic compounds present in the natural Amazonian aerosol:
993 Characterization by gas chromatography-mass spectrometry: Organic compounds in
994 Amazonian aerosols., *J. Geophys. Res. Atmospheres*, 108(D24), 4766, 2003.
- 995 Grange, S. K., Fischer, A., Zellweger, C., Alastuey, A., Querol, X., Jaffrezo, J. L., Uzu, G.,
996 and Hueglin, C.: Switzerland's PM₁₀ and PM_{2.5} environmental increments show the
997 importance of non-exhaust emissions, *Atmos. Environ.*, submitted (on 22/06/21).
- 998 Hansen, A.D., Rosen, H. and Novakov, T.: The Aethalometer: An Instrument for the Real Time
999 Measurement of Optical Absorption by Particles, *Sci. Tot. Environ.*, 36, 191–196,
1000 [https://doi.org/10.1016/0048-9697\(84\)90265-1](https://doi.org/10.1016/0048-9697(84)90265-1), 1984.
- 1001 Jaenicke, R.: Abundance of cellular material and proteins in the atmosphere, *Science*,
1002 308(5718), 73–73, <https://doi.org/10.1126/science.1106335>, 2005.
- 1003 Jaffrezo, J. L., Calas, N., and Bouchet, M.: Carboxylic acids measurements with ionic
1004 chromatography, *Atmos. Environ.*, 32(14), 2705–2708, 1998.
- 1005 Jia, Y., Bhat, S., and Fraser, M. P.: Characterization of saccharides and other organic
1006 compounds in fine particles and the use of saccharides to track primary biologically derived
1007 carbon sources, *Atmos. Environ.*, 44(5), 724–732, 2010a.

- 1008 Karagulian, F., Belis, C. A., Dora, C. F. C., Prüss-Ustün, A. M., Bonjour, S., Adair-Rohani,
1009 and H., Amann, M.: Contributions to cities' ambient particulate matter (PM): A systematic
1010 review of local source contributions at global level, *Atmos. Environ.*, 120, 475–483, 2015.
- 1011 Klimont, Z., Kupiainen, K., Heyes, C., Purohit, P., Cofala, J., Rafaj, P., Borken-Kleefeld, J.,
1012 and Schöpp, W.: Global anthropogenic emissions of particulate matter including black carbon,
1013 *Atmos. Chem. Phys.*, 17, 8681–8723, 2017.
- 1014 Kunit, M., and Puxbaum, H.: Enzymatic determination of the cellulose content of atmospheric
1015 aerosols, *Atmos. Environ.*, 30, 1233–1236, 1996.
- 1016 Liang, L., Engling, G., Du, Z., Cheng, Y., Duan, F., Liu, X., and He, K.: Seasonal variations
1017 and source estimation of saccharides in atmospheric particulate matter in Beijing, China,
1018 *Chemosphere*, 150, 365–377, 2016.
- 1019 Liu, C., Berg, B., Kutsch, W., Westman, C. J., Ilvesniemi, H., Shen, X., Shen, G., and Chen,
1020 X.: Leaf litter nitrogen concentration as related to climatic factors in Eurasian forests, *Global
1021 Ecology and Biogeography*, 15, 438–444, 2006.
- 1022 Madsen, D., Azeem, H. A., Sandahl, M., van Hees, P., and Husted, B.: Levoglucosan as a
1023 Tracer for Smouldering Fire, *Fire Technology*, 54, 1871–1885, 2018.
- 1024 Martin, S. T., Andreae, O. M., Artaxo, P., Baumgardner, D., Chen, Q., Goldenstein, A. H.,
1025 Guenther, A., Heald, C. L., Mayol-Bracero, O. L., McMurry, P. H., Pauliquevis, T., Pöschl,
1026 U., Prather, K. A., Roberts, G. C., Saleska, S. R., Silva Dias, M. A., Spracklen, D. V.,
1027 Swietlicki, E., and Trebs, I.: Sources and properties of Amazonian aerosol particles, *Rev.
1028 Geophys.*, 48(2), <https://doi.org/10.1029/2008RG000280>, 2010.
- 1029 Martínez, A., Larrañaga, A., Pérez, J., Descals, E., and Pozo, J.: Temperature affects leaf litter
1030 decomposition in low-order forest streams: field and microcosm approaches, *FEMS Microb.
1031 Ecol.*, 87, 257–267, 2014.
- 1032 Medeiros, P. M., Conte, M. H., Weber, J. C., and Simoneit, B. R. T.: Sugars as source indicators
1033 of biogenic organic carbon in aerosols collected above the Howland Experimental Forest,
1034 Maine, *Atmos. Environ.*, 40(9), 1694–1705, 2006.
- 1035 Michoud, V., Hallemans, E., Chiappini, L., Leoz-Garziandia, E., Colomb, A., Dusanter, S.,
1036 Fronval, I., Gheusi, F., Jaffrezo, J. L., Léonardis, T., Locoge, N., Marchand, N., Sauvage, S.,
1037 Sciare, J., and Doussin, J. F.: Molecular characterization of gaseous and particulate oxygenated
1038 compounds at a remote site in Cape Corsica in the western Mediterranean basin, *Atmos. Chem.
1039 Phys.*, 21(10), 8067–8088, <https://doi.org/10.5194/acp-21-8067-2021>, 2021.
- 1040 Mobil'Air QAMECS Program: [https://mobilair.univ-grenoble-alpes.fr/mobilair/projets-
1041 associes/projets-associes-743738.htm?RH=2206232030103086](https://mobilair.univ-grenoble-alpes.fr/mobilair/projets-associes/projets-associes-743738.htm?RH=2206232030103086), last access: 13 April 2021.
- 1042 Nozière, B., Kalberer, M., Claeys, M., Allan, J., D'Anna, B., Decesari, S., Finessi, E., Glasius,
1043 M., Grgić, I., Hamilton, J. F., Hoffmann, T., Iinuma, Y., Jaoui, M., Kahnt, A., Kampf, C. J.,
1044 Kourtchev, I., Maenhaut, W., Marsden, N., Saarikoski, S., Schnelle-Kreis, J., Surratt, J. D.,
1045 Szidat, S., Szmigielski, R., and Wisthaler, A.: The molecular identification of organic

- 1046 compounds in the atmosphere: state of the art and challenges, *Chem. Rev.*, 115(10), 3919–
1047 3983, <https://doi.org/10.1021/cr5003485>, 2015.
- 1048 OPE-ANDRA Atmospheric Station: <http://ope.andra.fr/index.php?lang=fr>, last access: 6
1049 January 2021.
- 1050 Peccia, J., Hospodsky, D., and Bibby, K.: New Directions : A revolution in DNA sequencing
1051 now allows for the meaningful integration of biology with aerosol science, *Atmos. Environ.*,
1052 45, 1896–1897, 2011.
- 1053 Penner, J. E., Andreae, M., Annegarn, H., Barrie, L., Feichter, J., Hegg, D., Jayaraman, A.,
1054 Leaitch, R., Murphy, D., Nganga, J., and Pitari, G.: *Aerosols, their Direct and Indirect Effects,*
1055 *Climate Change 2001: The Scientific Basis.*, Cambridge University Press, Cambridge, 2001.
- 1056 Pöschl, U., Martin, S. T., Sinha, B., Chen, Q., Gunthe, S. S., Huffman, J. A., Borrmann, S.,
1057 Farmer, D. K., Garland, R. M., Helas, G., Jimenez, J. L., King, S. M., Manzi, A., Mikhailov,
1058 E., Pauliquevis, T., Petters, M. D., Prenni, A. J., Roldin, P., Rose, D., Schneider, J., Su, H.,
1059 Zorn, S. R., Artaxo, P., and Andreae, M. O.: Rainforest Aerosols as Biogenic Nuclei of Clouds
1060 and Precipitation in the Amazon, *Science*, 329 (5998), 1513–1516, 2010.
- 1061 Pöschl, U.: Atmospheric Aerosols: Composition, Transformation, Climate and Health Effects,
1062 *Angew. Chem. Int. Ed.*, 44(46), 7520 – 7540, 2005.
- 1063 Putaud, J.-P., Raes, F., Van Dingenen, R., Brüggemann, E., Facchini, M.-C., Decesari, S.,
1064 Fuzzi, S., Gehrig, R., Hüglin, C., Laj, P., Lorbeer, G., Maenhaut, W., Mihalopoulos, N., Müller,
1065 K., Querol, X., Rodriguez, S., Schneider, J., Spindler, G., Brink, H. ten, Tørseth, K., and
1066 Wiedensohler, A.: A European aerosol phenomenology 2: chemical characteristics of
1067 particulate matter at kerbside, urban, rural and background sites in Europe, *Atmos. Environ.*,
1068 38(16), 2579–2595, 2004a.
- 1069 Putaud, J.-P., Van Dingenen, R., Alastuey, A., Bauer, H., Birmili, W., Cyrys, J., Flentje, H.,
1070 Fuzzi, S., Gehrig, R., Hansson, H. C., Harrison, R. M., Herrmann, H., Hitzenberger, R., Hüglin,
1071 C., Jones, A. M., Kasper-Giebl, A., Kiss, G., Koussa, A., Kuhlbusch, T. A. J., Löschau, G.,
1072 Maenhaut, W., Molnar, A., Moreno, T., Pekkanen, J., Perrino, C., Pitz, M., Puxbaum, H.,
1073 Querol, X., Rodriguez, S., Salma, I., Schwarz, J., Smolik, J., Schneider, J., Spindler, G., ten
1074 Brink, H., Tursic, J., Viana, M., Wiedensohler, A. and Raes, F.: A European aerosol
1075 phenomenology – 3: Physical and chemical characteristics of particulate matter from 60 rural,
1076 urban, and kerbside sites across Europe, *Atmos. Environ.*, 44(10), 1308–1320,
1077 <https://doi.org/10.1016/j.atmosenv.2009.12.011>, 2010.
- 1078 Puxbaum, H., and Tenze-Kunit, M.: Size distribution and seasonal variation of atmospheric
1079 cellulose, *Atmos. Environ.*, 37(26), 3693–3699, 2003.
- 1080 Rogge, W. F., Mazurek, M. A., Hildemann, L. M., Cass, G. R., and Simoneit, B. R. T.:
1081 Quantification of urban organic aerosols at a molecular level: identification, abundance and
1082 seasonal variation, *Atmos. Environ.*, 27(8), 1309–1330, [https://doi.org/10.1016/0960-](https://doi.org/10.1016/0960-1686(93)90257-Y)
1083 1686(93)90257-Y, 1993a.

- 1084 Rogge, W. F., Mazurek, M. A., Hildemann, L. M., Cass, G. R., and Simoneit, B. R. T.: Sources
1085 of fine organic aerosol. 4. particulate abrasion products from leaf surfaces of urban plants,
1086 *Environ. Sci. Technol.*, 27(13), 2700–2711, <https://doi.org/10.1021/es00049a008>, 1993b.
- 1087 Rosenfeld, D., Lohmann, U., Raga, G. B., O’Dowd, C. D., Kulmala, M., Fuzzi, S., Reissell,
1088 A., and Andreae, M. O.: Flood or Drought: How Do Aerosols Affect Precipitation?, *Science*,
1089 321(5894), 1309–1313, 2008.
- 1090 Samaké, A., Jaffrezo, J.-L., Favez, O., Weber, S., Jacob, V., Albinet, A., Riffault, V., Perdrix,
1091 E., Waked, A., Golly, B., Salameh, D., Chevrier, F., Oliveira, D. M., Bonnaire, N., Besombes,
1092 J.-L., Martins, J. M. F., Conil, S., Guillaud, G., Mesbah, B., Rocq, B., Robic, P.-Y., Hulin, A.,
1093 Le Meur, S., Descheemaeker, M., Chretien, E., Marchand, N. and Uzu, G.: Polyols and
1094 glucose particulate species as tracers of primary biogenic organic aerosols at 28 French sites,
1095 *Atmos. Chem. Phys.*, 19(5), 3357–3374, <https://doi.org/10.5194/acp-19-3357-2019>, 2019a.
- 1096 Samaké, A., Jaffrezo, J.-L., Favez, O., Weber, S., Jacob, V., Albinet, A., Riffault, V., Perdrix, E.,
1097 Waked, A., Golly, B., Salameh, D., Chevrier, F., Oliveira, D. M., Bonnaire, N., Besombes, J.-L.,
1098 Martins, J. M. F., Conil, S., Guillaud, G., Mesbah, B., Rocq, B., Robic, P.-Y., Hulin, A., Le Meur,
1099 S., Descheemaeker, M., Chretien, E., Marchand, N. and Uzu, G.: Polyols and glucose as tracers
1100 of primary biogenic organic aerosol: influence of environmental factors on ambient air
1101 concentrations and spatial distribution over France, *Atmos. Chem. Phys.*, [https://doi.org](https://doi.org/10.5194/acp-19-11013-2019)
1102 [/10.5194/acp-19-11013-2019](https://doi.org/10.5194/acp-19-11013-2019), 2019b.
- 1103 Samaké, A., Bonin, A., Jaffrezo, J. L., Taberlet, P., Uzu, G., Jacob, V., Conil, S., and Martins,
1104 J. M. F.: High levels of Primary Biogenic Organic Aerosols in the atmosphere in summer are
1105 driven by only a few microorganisms from the leaves of surrounding plants, *Atmos. Chem.*
1106 *Phys.*, <https://doi.org/10.5194/acp-20-5609-2020>, 2020.
- 1107 Samake, A., Martins, J. M., Bonin, A., Uzu, G., Taberlet, P., Conil, S., Favez, O., Thomasson,
1108 A., Chazeau, B., Marchand, N., and Jaffrezo, J. L.: Variability of the atmospheric PM₁₀
1109 microbiome in three climatic regions of France, *Frontiers in Microbiology*, [https://doi.org](https://doi.org/10.3389/fmicb.2020.576750)
1110 [10.3389/fmicb.2020.576750](https://doi.org/10.3389/fmicb.2020.576750), 2021.
- 1111 Sánchez-Ochoa, A., Kasper-Giebl, A., Puxbaum, H., Gelencsér, A., Legrand, M., and Pio, C.:
1112 Concentration of atmospheric cellulose: A proxy for plant debris across a west-east transect
1113 over Europe, *J. Geophys. Res.*, 112, <https://doi.org/10.1029/2006JD008180>, 2007.
- 1114 Simoneit, B. R. T., and Mazurek, M. A.: Organic matter of the troposphere—II. Natural
1115 background of biogenic lipid matter in aerosols over the rural western united states, *Atmos.*
1116 *Environ.*, 16(9), 2139–2159, [https://doi.org/10.1016/0004-6981\(82\)90284-0](https://doi.org/10.1016/0004-6981(82)90284-0), 1982.
- 1117 Schmidl, C.: PM₁₀—Quellenprofile von Holzrauchemissionen aus Kleinf Feuerungen,
1118 Diplomarbeit, Inst. für Chem. Technol. und Analytik, Tech. Univ. Wien, Vienna, 2005.
- 1119 Verma, S. K., Kawamura, K., Chen, J., and Fu, P.: Thirteen years of observations on primary
1120 sugars and sugar alcohols over remote Chichijima Island in the western North Pacific, *Atmos.*
1121 *Chem. Phys.*, 18(1), 81–101, 2018.

- 1122 Waked, A., Favez, O., Alleman, L. Y., Piot, C., Petit, J.-E., Delaunay, T., Verlinden, E., Golly,
1123 B., Besombes, J.-L., Jaffrezo, J.-L., and Leoz-Garziandia, E.: Source apportionment of PM10
1124 in a north-western Europe regional urban background site (Lens, France) using positive matrix
1125 factorization and including primary biogenic emissions, *Atmos. Chem. Phys.*, 14(7), 3325–
1126 3346, 2014.
- 1127 Wagenbrenner, N. S., Chung, S. H., and Lamb, B. K.: A large source of dust missing in
1128 Particulate Matter emission inventories? Wind erosion of post-fire landscapes, *Elem. Sci.*
1129 *Anth.*, 5(2), <https://doi.org/10.1525/elementa.185>, 2017.
- 1130 Weber, S., Salameh, D., Albinet, A., Alleman, L. Y., Waked, A., Besombes, J.-L., Jacob, V.,
1131 Guillaud, G., Meshbah, B., Rocq, B., Hulin, A., Dominik-Sègue, M., Chrétien, E., Jaffrezo, J.-
1132 L. and Favez, O.: Comparison of PM10 Sources Profiles at 15 French Sites Using a
1133 Harmonized Constrained Positive Matrix Factorization Approach, *Atmosphere*, 10(6), 310,
1134 <https://doi.org/10.3390/atmos10060310>, 2019.
- 1135 Winiwarter, W., Bauer, H., Caseiro, A., and Puxbaum, H.: Quantifying emissions of primary
1136 biological aerosol particle mass in Europe, *Atmos. Environ.*, 43, 1403–1409, 2009.
- 1137 Wu, C. and Yu, J. Z.: Determination of primary combustion source organic carbon-to-
1138 elemental carbon (OC/EC) ratio using ambient OC and EC measurements: secondary OC-EC
1139 correlation minimization method, *Atmos. Chem. Phys.*, 16, 5453–5465, 2016.
- 1140 Yttri, K. E., Aas, W., Bjerke, A., Cape, J. N., Cavalli, F., Ceburnis, D., Dye, C., Emblico, L.,
1141 Facchini, M. C., Forster, C., Hanssen, J. E., Hansson, H. C., Jennings, S. G., Maenhaut, W.,
1142 Putaud, J. P., and Tørseth, K.: Elemental and organic carbon in PM10: a one year
1143 measurement campaign within the European Monitoring and Evaluation Programme EMEP,
1144 *Atmos. Chem. Phys.*, 7, 5711–5725, <https://doi.org/10.5194/acp-7-5711-2007>, 2007.
- 1145 Yttri, K. E., Simpson, D., Stenström, K., Puxbaum, H. and Svendby, T.: Source apportionment
1146 of the carbonaceous aerosol in Norway – quantitative estimates based on ¹⁴C, thermal-optical
1147 and organic tracer analysis, *Atmos. Chem. Phys. Discuss.*, 11(3), 7375–7422, 2011a.
- 1148 Yttri, K. E., Simpson, D., Nøjgaard, J. K., Kristensen, K., Genberg, J., Stenström, K.,
1149 Swietlicki, E., Hillamo, R., Aurela, M., Bauer, H., Offenberg, J. H., Jaoui, M., Dye, C.,
1150 Eckhardt, S., Burkhardt, J. F., Stohl, A., and Glasius, M.: Source apportionment of the summer
1151 time carbonaceous aerosol at Nordic rural background sites, *Atmos. Chem. Phys.*, 11, 13339 –
1152 13357, 2011b.
- 1153 Zhang, T., Engling, G., Chan, C. Y., Zhang, Y. N., Zhang, Z. S., Lin, M., Sang, X. F., Li, Y.
1154 D., and Li, Y. S.: Contribution of fungal spores to particulate matter in a tropical rainforest,
1155 *Environ. Res. Lett.*, 5(2), 24010, 2010.
- 1156 Zhu, C., Kawamura, K., and Kunwar, B.: Organic tracers of primary biological aerosol
1157 particles at subtropical Okinawa Island in the western North Pacific Rim: Organic biomarkers
1158 in the north pacific, *J. Geophys. Res. Atmospheres*, 120(11), 5504–5523, 2015.